Received: 28 August 2020 | Revised: 31 December 2022 | Accepted: 4 January 2023

DOI: 10.1111/jnc.15767

Journal of Neurochemistry JNC The Official Journal of the International Society for Neurochemistry WILEY

ORIGINAL ARTICLE

Hericerin derivatives activates a pan-neurotrophic pathway in central hippocampal neurons converging to ERK1/2 signaling enhancing spatial memory

Ramón Martínez-Mármol[1] | YeJin Chai[1] | Jacinta N. Conroy[2] | Zahra Khan[3] | Seong-Min Hong[3] | Seon Beom Kim[4] | Rachel S. Gormal[1] | Dae Hee Lee[5] | Jae Kang Lee[5] | Elizabeth J. Coulson[1,2] | Mi Kyeong Lee[4] | Sun Yeou Kim[3,6] | Frédéric A. Meunier[1,2]

[1]Clem Jones Centre for Ageing Dementia Research, Queensland Brain Institute, The University of Queensland, Brisbane, Queensland, Australia

[2]School of Biomedical Sciences, The University of Queensland, Brisbane, Queensland, Australia

[3]College of Pharmacy, Gachon University, Incheon, Republic of Korea

[4]College of Pharmacy, Chungbuk National University, Cheongju, Republic of Korea

[5]CNGBio corp, Cheongju-si, Chungcheongbuk-do, Republic of Korea

[6]Gachon Institute of Pharmaceutical Science, Gachon University, Incheon, Republic of Korea

Correspondence
Frédéric A. Meunier, Queensland Brain Institute, The University of Queensland, Brisbane, Qld. 4072, Australia.
Email: f.meunier@uq.edu.au

Funding information
NHMRC Senior Research Fellowship, Grant/Award Number: GNT1155794; Clem Jones Foundation; National Research Foundation of Korea; Australian Research Council LIEF Grant, Grant/Award Number: LE130100078; State Government of Queensland; NHMRC

Abstract

The traditional medicinal mushroom *Hericium erinaceus* is known for enhancing peripheral nerve regeneration through targeting nerve growth factor (NGF) neurotrophic activity. Here, we purified and identified biologically new active compounds from *H. erinaceus*, based on their ability to promote neurite outgrowth in hippocampal neurons. *N*-de phenylethyl isohericerin (NDPIH), an isoindoline compound from this mushroom, together with its hydrophobic derivative hericene A, were highly potent in promoting extensive axon outgrowth and neurite branching in cultured hippocampal neurons even in the absence of serum, demonstrating potent neurotrophic activity. Pharmacological inhibition of tropomyosin receptor kinase B (TrkB) by ANA-12 only partly prevented the NDPIH-induced neurotrophic activity, suggesting a potential link with BDNF signaling. However, we found that NDPIH activated ERK1/2 signaling in the absence of TrkB in HEK-293T cells, an effect that was not sensitive to ANA-12 in the presence of TrkB. Our results demonstrate that NDPIH acts via a complementary neurotrophic pathway independent of TrkB with converging downstream ERK1/2 activation. Mice fed with *H. erinaceus* crude extract and hericene A also exhibited increased neurotrophin expression and downstream signaling, resulting in significantly enhanced hippocampal memory. Hericene A therefore acts through a novel pan-neurotrophic signaling pathway, leading to improved cognitive performance.

KEYWORDS
BDNF, hericerin, *Hericium erinaceus*, memory, neurite outgrowth, TrkB

Abbreviations: A1, ethanol extract; A2, CH_2Cl_2-soluble extract; A2-C2, hericene A; A2-C3, corallocin A; A2-C4, 4-[3′,7′-dimethyl-2′,6′-octadienyl]-2-formyl-3-hydroxy-5-methyoxybenzylalcohol; A3, EtOAc-soluble extract; A4, n-BuOH soluble extract; A5, water soluble extract; A6, water fraction extract from the filter cake; ANA-12, N-[2-[[(Hexahydro-2-oxo-1H-azepin-3-ylamino]carbonyl]phenyl]benzo[b]thiophene-2-carboxamide; BBB, blood–brain barrier; BDNF, brain-derived neurotrophic factor; CNS, central nervous system; CREB, cAMP response element-binding protein; DIV, days in vitro; DMSO, dimethyl sulfoxide; E, embryonic day; ERK1/2, extracellular signal-regulated kinase 1/2; NDPIH, N-de phenylethyl isohericerin; NGF, nerve growth factor; NORT, novel object recognition task test; NT3, neurotrophin 3; NT4/5, neurotrophin 4/5; PKB, Akt, protein kinase B; TrkA, tropomyosin receptor kinase A; TrkB, tropomyosin receptor kinase B.

Ramón Martínez-Mármol, YeJin Chai, Jacinta N. Conroy, Zahra Khan contributed equally to this work.

Boosting Dementia Research Initiative; Medical Research Centre program, Grant/Award Number: 2017R1A5A2015541; National Research Foundation of Korea; CNG-Bio grant

1 | INTRODUCTION

Neurotrophins are a family of molecules that promote neuronal survival, neurite outgrowth, and dendritic branching through binding specificity for particular tropomyosin receptor kinase (Trk) and p75 neurotrophin receptors (Kaplan & Miller, 2000). The mammalian neurotrophin family is comprised of nerve growth factor (NGF), brain-derived neurotrophic factor (Ip et al., 1993) (BDNF), neurotrophin 3 (NT3) and neurotrophin 4/5 (NT4/5) (Chao, 2003; Ip et al., 1993). Both NGF and BDNF neurotrophins also bind to p75 receptor which when expressed together with Trk receptors can promote its high affinity ligand interactions and enhanced trophic signaling resulting in neuronal survival, neurite outgrowth and synaptogenesis (Kaplan & Miller, 2000). BDNF in particular, is highly expressed in the adult central nervous system (CNS) and is critically important for the function of neurons located in areas of the brain involved in memory acquisition such as the hippocampus and the cortex (Allen et al., 2011). BDNF and its receptor TrkB are essential for long-term potentiation, an Hebbian mechanism strengthening synaptic output in response to a high frequency train of stimulation, as well as learning (Allen et al., 2011; Minichiello et al., 1999).

Dysfunction of the BDNF pathway has been linked with several disorders of the brain, including Alzheimer's disease (Allen et al., 2011), schizophrenia (Xiu et al., 2009), Huntington's disease (Zuccato & Cattaneo, 2009), and Rett syndrome (Zuccato & Cattaneo, 2009). Not surprisingly, neurotrophins and their receptors have been identified as targets for the therapeutic treatment of a range of neurodegenerative and neurological disorders (Nagahara & Tuszynski, 2011). However, exogenous neurotrophin-based treatments have failed clinical trials for a variety of reasons including short half-life, poor blood–brain barrier (BBB) permeability, and off-target effects (Chan et al., 2017; Nagahara & Tuszynski, 2011).

Alternative interventions that increase endogenous BDNF levels or enhance TrkB activity through lifestyle and/or botanical supplements, are also an area of great interest. Ongoing efforts are made to identify compounds derived from natural sources. Traditional Chinese medicine provides an enticing source of potential botanical remedies, with several common drugs stemming from the Chinese pharmacopeia having been used for millennia throughout Asia and India because of their therapeutic or poisonous pharmacologic profiles.

A promising nootropic fungus, known for its neurotrophic profile, comes from *Hericium erinaceus*, also known as Lion's Mane mushroom, which, paradoxically, was used to treat unrelated ailments such as stomach aches and as prophylactic treatment of cancers (Kim et al., 2013). Several studies have reported strong neurotrophic effects, along with the identification of numerous bioactive components, including polysaccharides, erinacines, hericerins, alkaloids, steroids and many others (Brandalise et al., 2017; Friedman, 2015). Interestingly, hericenones and erinacines can effectively cross the BBB (Hu et al., 2019) and exhibit neuroprotective effects both in vitro and to in vivo in animal models of peripheral nerve injury (Wong et al., 2012), and in conditions of the brain including stroke (Hazekawa et al., 2010) and Alzheimer's disease (Friedman, 2015; Kawagishi & Zhuang, 2008; Mori et al., 2011).

Compounds derived from *H. erinaceus* extracts have been shown to promote NGF synthesis and secretion (Kawagishi et al., 1996; Lai et al., 2013; Mori et al., 2009; Raman et al., 2015; Zhang et al., 2015) and to act via the TrkA pathway involving MEK/ERK and PI3K/Akt activation (Haure-Mirande et al., 2017; Phan et al., 2014). However, the NGF/TrkA-mediated neuroprotective effects predominantly focus on neurons in the peripheral nervous system (Ustun & Ayhan, 2019). More recently, *H. erinaceus* extract has been suggested to also affect the BDNF pathway in 1321 N1 human astrocytoma cell line (Rupcic et al., 2018), in the mouse brain (Chiu et al., 2018) and to promote increasing circulating pro-BDNF levels in humans (Vigna et al., 2019). It is therefore possible that *H. erinaceus* extract can affect TrkB-dependent central neuronal function.

To test this idea, we purified and identified several compounds and tested their ability to influence TrkB signaling and neuronal morphology in hippocampal neurons. Treatment with *H. erinaceus* extracts increased neurite outgrowth and branching, and super-resolution structured illumination microscopy revealed much enlarged growth cone morphology. This neurotropic effect was partially blocked by the TrkB inhibitor ANA-12. We further found that dietary supplementation with *H. erinaceus* crude extract significantly enhanced recognition memory. Importantly, supplementation with 20–50 times lower concentration of purified hericene A was equally potent at enhancing recognition memory. Tested rodents exhibited elevated BDNF and TrkB downstream activation effectors levels. However, NDPIH activated ERK1/2 signaling in the absence of TrkB expression in HEK-293T cells, an effect that was not inhibited by ANA-12. We concluded that hericene A acts via an unknown complementary pathway to increase ERK1/2 signaling. Overall, our results demonstrate that hericene A is a potent memory enhancer that act via a novel signaling pathway converging on ERK1/2 signaling pathway.

2 | MATERIALS AND METHODS

The authors state that the study was not pre-registered.

2.1 | Preparation of samples

The fruiting bodies of *H. erinaceus* were provided from the C&G Agricultural Association (Sejong, Korea). Column chromatography was

performed on silica gel (Kieselgel 60, 70–230 mesh, Merck), and semi-preparative HPLC was performed using a Waters HPLC system (Waters) equipped with two Waters 515 pumps with a 2996 photodiode-array detector. The dried fruiting body of *H. erinaceum* was extracted with EtOH at room temperature and filtered with filter paper, which yielded the ethanol extract (A1) and filter cake. The ethanol extract was suspended in H_2O and partitioned with CH_2Cl_2, EtOAc, *n*-BuOH, successively, to yield the CH_2Cl_2-soluble (A2), EtOAc-soluble (A3), *n*-BuOH soluble (A4) and water fraction (A5). The filter cake was further extracted with water to yield water extract (A6). The CH_2Cl_2-soluble fraction (A2) was chromatographed on silica gel eluting with a mixture of *n*-hexane-EtOAc by step gradient to give 12 subfractions (A2A-A2L). C1 and C3 were obtained from A2F and A2K, respectively, by semi-preparative HPLC eluting with MeCN-water (45:55). C2 and C4 were obtained from A2D by recrystallisation followed by semi-preparative HPLC eluting with MeCN. The structures of isolated compounds were identified as *N*-de phenylethyl isohericerin (C1), hericene A (C2), corallocin A (C3) and 4-[3′, 7′-dimethyl-2′,6′-octadienyl]-2-formyl-3-hydroxy-5-methyoxybenzylalcohol (C4) by the analysis of the spectroscopic data and comparison with literature values (Li et al., 2015; Wittstein et al., 2016).

2.2 | Reagents

Extracts from Lion's mane mushroom and Ginkgo leaves were weight and dissolved in dimethyl sulfoxide (DMSO) (Merck, cat. no. D8418) to obtain stock solutions concentrated at 0.1, 1 and 10 mg/mL. Working solutions of the extracts were prepared by diluting 1:1000 the stocks in neurobasal medium at the following concentrations 0 μg/mL, 0.1 μg/mL, and 10 μg/mL. Hippocampal neurons at DIV2 (2 days in vitro) or DIV3 were incubated with the extracts during 24 h. After the treatments (DIV3 or DIV4), neurons were prepared for immunocytochemistry. Recombinant human BDNF and ANA-12 (Sigma-Aldrich, cat. no. SML0209) was incubated during 24 h at 1 nM and 50 μM, respectively. Recombinant human BDNF (Gibco-Thermo Fisher, cat. no. PHC7074) was incubated for 1 h at 36 pM (1 ng/mL) or 1.4 nM (40 ng/mL).

2.3 | HEK-293T cell culture

HEK-293T cells were cultured in DMEM medium (GIBCO-Thermo Fisher Scientific, cat. no. 21969-035) supplemented with 10% fetal bovine serum (FBS) (Gibco-Thermo Fisher, cat. no. 26140–079) at 37°C, 5% CO_2. This cell line is not listed as commonly misidentified cell line by the International Cell Line Authentication Committee (ICLAC; http://iclac.org/databases/cross-contaminations/). The HEK-293T cells used wer authenticated by the product vendor (American Type Culture Collection, ATCC, https://www.atcc.org/products/crl-11268). The cells were kept below 20 passages. Cells were plated and 48 h later transfected with 250 ng TrkB plasmid and 500 ng vector-control or $p75^{ICD}$ expression constructs using Lipofectamine 2000 (Invitrogen, cat. no. 11668027) as per manufacturer's protocol. The following day cells were serum starved and ANA-12 (50 μM) was added to appropriate wells 5 h prior to stimulation with either DMSO, G1 (purified NDPIH,10 μg/mL), G3 (unrelated mushroom extract, 10 μg/mL) or BDNF (1 ng/mL or 40 ng/mL). After 1 h of stimulation cells were harvested and prepared for Western Blot analysis.

2.4 | Primary hippocampal cultures

The procedures to obtain primary neurons from embryonic rats were carried out in accordance with the University of Queensland Animal Ethics Committee ethical guidelines and regulations. Permission to carry out the animal experiments described in this manuscript was given by the Anatomical Biosciences Animal Ethics Committee at the University of Queensland (approval reference 2019/AE000244). Hippocampal neurons were obtained from Sprague Dawley (SD) rats at embryonic day (E)18 and prepared as described previously (Joensuu et al., 2016, 2017). Twenty Adult pregnant female SD rats were used in this study. Briefly, pregnant E18 SD rat dams were sacrificed using the approved method of euthanasia, cervical dislocation. Brains from a minimum of 5 embryos were pooled before plating. Hippocampal neurons used were seeded at 20000 cells onto 35 mm poly-L-lysine-coated glass-bottom dishes (Cellvis, cat. no. D35-20-1.5 N) or coverslips in Neurobasal growth medium (Gibco-Thermo Fisher, cat. no. 21103–049) supplemented with 2% B27 (Gibco-Thermo Fisher, cat. no. 17504-044), 2 mM Glutamax (Gibco-Thermo Fisher, cat. no. 35050-061), 50 U/mL penicillin, 50 μg/mL streptomycin (Invitrogen-Thermo Fisher, cat. no. 15140-122), and 5% FBS (Wang et al., 2015, 2016, 2020). At 1 day in vitro (DIV1), neurons were switched to serum-free medium until fixation at DIV4. In specified studies, hippocampal neurons were seeded at lower density (10000 cells) in the complete absence of serum to avoid any interference and paracrine effect, and cultured for 2 days before being treated with specific reagents.

2.5 | Immunocytochemistry

Primary hippocampal neurons were fixed with, 4% paraformaldehyde (VWR, cat. no. 100503-914)/4% sucrose (Merk, cat. no. S0389) in PBS (Thermo Fisher Scientific, cat. no. 10010-023) for 10 min at room temperature, and permeabilized with, 0.1% Triton X-100 (Merk, cat. no. T8787) in PBS for 10 min. To detect the actin cytoskeleton, neurons were stained with a solution of 1 μg/mL Alexa-Fluor™ 647-phalloidin (Thermo Fisher, cat. no. A22287) in PBS for 60 min and rinsed with PBS, 3 times, 5 min each. Neurons were blocked for 1 h in PBS, 5% goat serum, 0.025% Triton X-100, followed by primary antibody incubation overnight at 4°C and secondary antibody incubation for 1 h at room temperature. The primary antibody used was mouse Anti-IIIβ-tubulin (Covance, cat. no. MMS-435P, 1:1000), and the secondary antibody was Alexa Fluor™ 488-labeled goat-anti-mouse or Alexa Fluor™ 555-labeled goat-anti-mouse (LifeTechnologies, Thermo Fisher, cat. no. A32723 and A32727 respectively, 1:500). Coverslips were mounted in ProLong medium (Thermo Fisher, cat. no. P36970). Fluorescence images were acquired with a 20× (0.8 NA / 550 μm WD / 0.22 μm/

pixel), or 63× (1.4 NA / 190 μm WD / 0.19 μm/pixel) objective on a Zeiss LSM510 META confocal microscope. Structured Illumination Microscopy (SIM) was performed on a Zeiss PS1 ELYRA equipped with a 63× (1.4 NA / Plan-Apochromat / 190 μm working distance / 0.064 μm/pixel/ Oil – For SIM) objective and a PCO scientific sCMOS camera. Images were acquired with an exposure time of 200 ms, a SIM grating size of 28 μm, using three rotations and 5 phases. Structured illumination images were then processed using Zen software.

2.6 | Image analysis and quantification of primary hippocampal neuron experiments

Each experiment contains a mixed culture of neurons isolated from a pool of five embryos. All experiments were repeated three times (different dissections). Between 30 and 60 selected neurons were acquired and analyzed blindly for each condition (the experimenter was unaware of the group during image acquisition and analysis). For the analysis of axon length, the longest neurite of each neuron was selected. Neurite Tracer tool from FIJI-ImageJ (Schindelin et al., 2012) software was used to quantify the length of the axons, the number of neurites and growth cone area.

2.7 | Behavior tests of animals and sample administration

Wild-type Institute of Cancer Research (ICR) male mice (23–25 g, 6 weeks old), were purchased from Orient Bio Co., and fed on a laboratory diet (AIN-76A purified diet) and given water ad libitum. 50 Adult ICR male mice were used in this study. Mice were housed for 1 week at 23 ± 1°C with 55 ± 5% humidity under a 12 h light/dark cycle. The Gachon University Lab Animal Care Committee approved the care and use of the mice for the study (approval reference GIACUC-R2019001) in accordance with the Korean Guide for Care and Use of Laboratory Animals. The mice were divided into four groups (10 mice per group) as followed: Vehicle group, piracetam group (positive control, PC), A1 group and A2-C2 group. The normal (10 mL/kg of distilled water, per os, *p.o.*), PC (400 mg/kg, p.o.), A1 (100 and 250 mg/kg, *p.o.*) or A2-C2 (5 mg/kg, *p.o.*) groups received oral administration of the substances, and each sample were dissolved in distilled water. Behavioral tests (Y-maze test and novel object recognition test) were conducted blindly, were performed on days 28–30, and mice were sacrificed on day 31 and the brains were used for biochemical and immunohistochemistry analysis (Figure 8a). Animals were sacrificed by CO_2 followed by additional cervical dislocation.

2.8 | Y-maze test

The Y-shaped maze consisted of three identical arms (60 × 15 × 12 cm^3) made of dark gray plastic with equal angles between each arm. The three arms of Y shape were marked as A, B and C. First, mice were placed into the centre of a Y-shaped runway and allowed to move throughout the maze for 8 min, and the move sequence (e.g., ABCCBA) and total number of arm entries was recorded manually (Bae et al., 2020). These parameters calculated included number of arm entries, same arm returns, alternate arm returns. The percentage of spontaneous alternation performance (%) was determined using equation (1). Equation (1) = [Actual alternations (total alternations)] / [Possible alternation (total number of arm entries – 2)] x 100.

2.9 | Novel object recognition task (NORT) test

The NORT test was performed by using an open box (60 × 60 × 60 cm^3) (Mesripour et al., 2016). Each mouse was place in the open box with two different kind of identical objects for 3 min on the first day for training. In the second day, each mouse was placed again in the box in which one of the identical objects had been replaced with a novel object. These parameters calculated included the time (in seconds) spent to explore the familiar object, time (in seconds) spent to explore the novel object, and total time (in seconds) spent to explore both objects. The percentage of recognition (%) was determined using equation (2). Equation (2) = [Time (in seconds) spent to explore the novel object] / [total time (in seconds) spent to explore both objects] x 100.

2.10 | Western blot analysis

HEK-293T cells were lysed into TNE (50 mM Tris–HCl, 100 mM NaCl, 0.1 mM EDTA) buffer containing 1%NP-40 (Thermo Fisher, cat. no. 85124), cOmplete, mini, EDTA-free protease inhibitor and PhosSTOP phosphatase inhibitor cocktail tables (Merk, cat. no. 04693159001). Protein concentration was determined using Peirce BCA assay (Thermo Fisher, cat. no. 23227) and normalized among samples. Total protein (30 μg) was separated on NuPAGE Bis-Tris 4–12% gels (Thermo Fisher, cat. no. NP0321), and then transferred to PVDF membrane (Thermo Fisher, cat. no. 88518). The transferred PVDF membranes were blocked with either 5% BSA in TBS/Tween 20 (0.1%) or 5% skim milk in TBS/Tween 20 (0.1%) for 1 h at room temperature. Membranes were then incubated at 4°C overnight with primary antibodies including extracellular-signal-regulated kinase (ERK), phosphorylated p-ERK (Thr202/Tyr204, CST cat. no. 9101, 1:1000), ERK1/2 (CST cat. no. 9102, 1:1000), p-TrkA (Y674/675)/p-TrkB (Y706/707) (CST cat. no. 4621, 1:500), TrkB (80E3, CST cat. no. 4603, 1:500), α-Tubulin (MP-Biomedicals cat. no. 91251, 1:2000), glyceraldehyde-3-phophate dehydrogenase (GAPDH, Abcam cat. no. ab9484, 1:1000), protein kinase B (Akt, CST cat. no. 9272, 1:1000) and p-Akt (CTS cat. no. 9271, 1:1000). The following day the membranes were incubated with secondary antibodies and proteins were visualized using Odyssey CLx (LI-COR Biosciences). Densitometric analysis was performed using LI-COR Image studio software.

Western blot assay for brain tissue ($n = 6$ brains per group) was performed as previously described (Subedi et al., 2019). The total proteins (30 μg) obtained from each brain tissue were separated by

10% acrylamide SDS-PAGE gel electrophoresis, and then transferred to PVDF membranes. The transferred PVDF membranes were incubated with primary antibodies (1:1000) including α-Tubulin (cat. no. T5168, Sigma), brain-derived neurotrophic factor (BDNF, cat. no. ANT010, Alomone Labs, Israel), nerve growth factor (NGF, cat. no. ab52918, Abcam), glial cell-derived neurotrophic factor (GDNF, cat. no. sc-13147, Santa cruz), tropomyosin receptor kinase A (TrkA, cat. no. 2510S, Cell Signaling Technology), phosphorylated (p)-TrkA (cat. no. 9141S, Cell Signaling Technology), tropomyosin receptor kinase B (TrkB, cat. no. 4603S, Cell Signaling Technology), p-TrkB (cat. no. PA5-36695, Invitrogen), extracellular-signal-regulated kinase (ERK, cat. no. 9695S, Cell Signaling Technology), p-ERK (cat. no. 9101S, Cell Signaling Technology), cAMP-response element binding protein (CREB, cat. no. 9197T, Cell Signaling Technology), p-CREB (cat. no. 9198S, Cell Signaling Technology) and synaptophysin (SYP, cat. No. sc-17750, Santa cruz) at 4°C overnight. On the second day, the membranes were incubated with secondary antibodies (1:2000), and protein bands were visualized using ECL Western Blotting Detection Reagents (Amersham Pharmacia Biotech, Little Chalfont,). Densitometric analysis was performed using Bio-Rad Quantity One software version 4.3.0 (Bio-Rad Laboratories, Inc.).

2.11 | Immunohistochemistry analysis

Whole brains ($n = 4$ brains per group) were collected from all groups and fixed in 10% formalin. The fixed brains were processed to obtain 40 μm-paraffin embedded sections. The obtained sections were deparaffinized using xylene and rehydrated with EtOH, followed by treatment with endogenous peroxidase blocker. After that the sections were washing within PBS and then incubated with the primary antibody, BDNF (dilution 1:100) at 4°C overnight. After 1 day, each section was incubated with a biotinylated anti-rabbit IgG (dilution 1:500) for 30 min and then with avidin-biotin horseradish peroxidase complex (Vector Laboratories). The optical density of BDNF immunoreactivity in dentate gyrus (DG) and cortex regions was analyzed via ImageJ software. The images were photographed at 10× magnification using a microscope (Olympus).

2.12 | Statistical analysis

All the values shown in the graphs represent the mean ± SEM. Statistical comparisons were performed on a per- neuron basis, per- cell culture preparation, per- brain or per- animal, as specified in the figure legends. No randomization was performed to allocate subjects in the study. No exclusion criteria were pre-determined. No animals were excluded or died during the experiments. No statistical methods were used to predetermine sample size but our sample sizes are similar to those reported in previous publications (Joensuu et al., 2016, 2017; Li et al., 2020). Sample size calculations can be found in Figure S10. All the results using hippocampal neuronal cultures were obtained from 2 to 4 neuronal dissections, pooling over 5 embryos per dissection. Results using cell lines were obtained from 3 experiments. The respective n values and the statistical test used in each experiment are specified in the corresponding figure legends and in Figure S11. Statistical tests were performed and figures were made using GraphPad Prism 7 software (GraphPad Software, Inc.). The D'Agostino and Pearson test was used to test for normality of acquired data. Two-tailed, unpaired Mann–Whitney *U* test was used to compare two conditions. One-way ANOVA with Tukey or Dunnett T3 post hoc test correction for multiple comparisons was used when the experiment compared more than two groups. Two-way ANOVA followed by Šidák post hoc test for multiple comparisons was also used when the experiment compared more than two groups. Significance is considered when p-value <0.05. The numerical value is provided in the graphs.

3 | RESULTS

To test the potential neurotrophic effect of *Hericium erinaceum* extracts, we performed various fractionations (Figure 1a) starting with an ethanol extract (A1), which was subsequently dried, resuspended in water and fractionated with dichloromethane (CH_2Cl_2) (A2) or further with ethyl acetate (EtOAc) (A3). The latter was further fractionated in *n*-butanol (*n*-BuOH) (A4) and in water (A5). Polysaccharide fraction (A6) was prepared from the filter cake after A1 was filtered. We dissolved all the fractions in DMSO and tested their effects on cultured hippocampal neurons. To carry out these experiments, hippocampal neurons from E18 rats were plated at relatively low density (20000 cells per coverslip) and cultured in the presence of FBS (5%) for 24 h. We then removed the serum and incubated them until DIV3, when we treated them with the extracts for 24 h prior to fixation and immunostaining processing with β-tubulin antibody (to visualize microtubules) and 4′,6-diamidino-2-phenylindole (DAPI, nuclear marker). The extract vehicle (DMSO) had no affect the axonal growth and neurite formation, (Figure 1b,c). However, Lion's Mane mushroom A2 extracts (1 μg/mL) resulted in a clear neurotrophic effect (Figure 1b,c) with axonal length increased by two-fold (Figure 1c). The number of neurites detected was also greatly increased by more than 3-fold (Figure 1c). Incubation of neuronal cultures with Lion's mane mushroom (A4-A6) extracts also triggered significant neurotrophic effects at concentrations of 1 μg/mL (Figure 1b,c), with axonal length increasing by several-fold (Figure 1c). The number of neurites detected was also greatly increased (Figure 1c).

A chloroform extract was then further fractionated by chromatography to further separate several molecules determined by NMR (Figure S1). Within this extraction, we identified *N*-de phenylethyl isohericerin (C1, NDPIH), hericene A (C2), corallocin A (C3), and 4-[3′,7′-dimethyl-2′,6′-octadienyl]-2-formyl-3-hydroxy-5-methyoxy benzylalcohol (C4) (Figure 2a). All of these purified extracts had significant neurotrophic activity as indicated by the 3-fold increase in neurite length and the increase in the number of neurites (Figure 2b,c and Figure S2). No pyknotic nuclei were observed suggesting that these compounds have no toxic effect at the concentrations used.

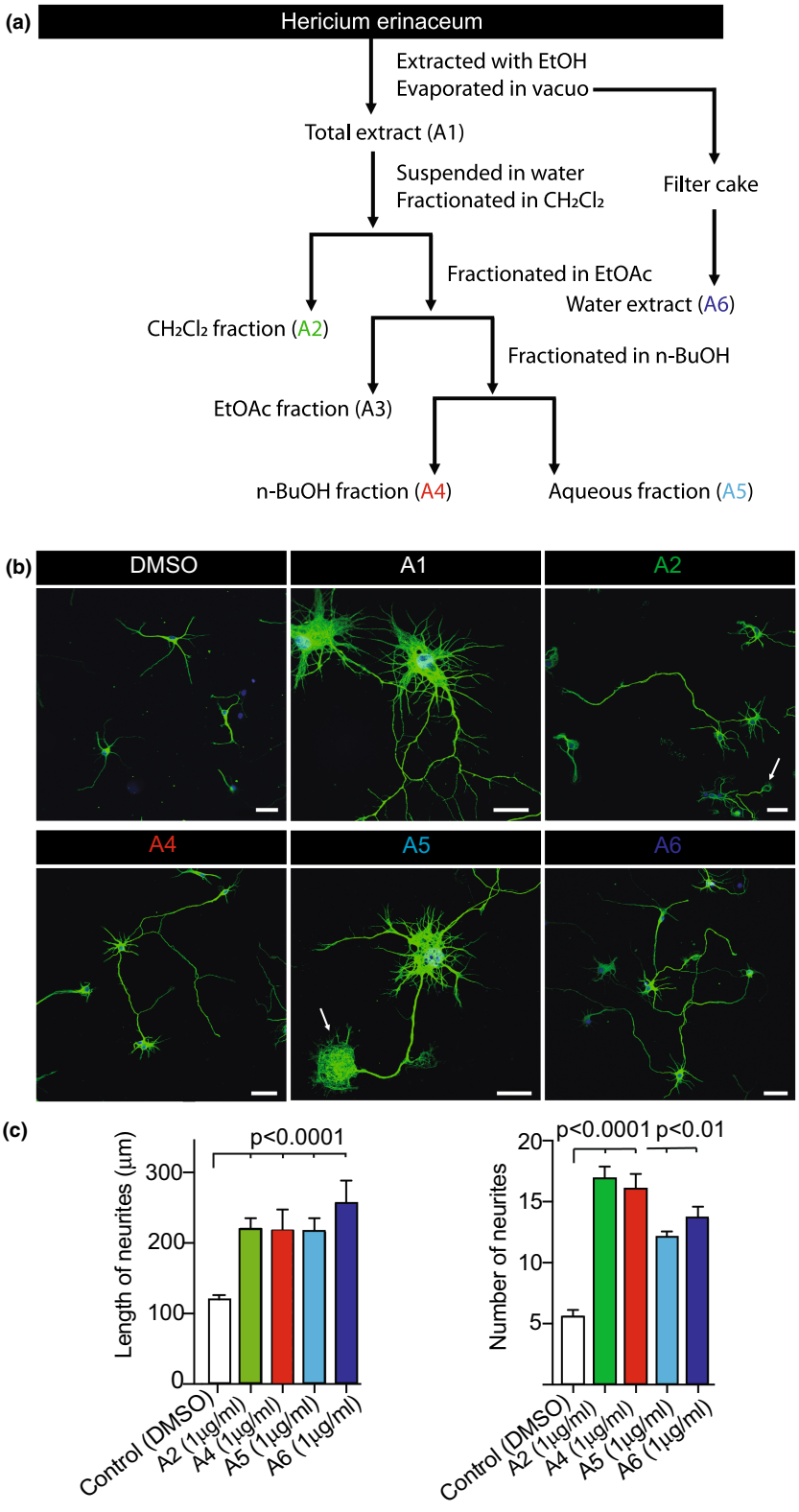

FIGURE 1 Lion's mane mushroom (LMM) extracts exert a potent neurotrophic effect in hippocampal neurons. (a) Scheme of the purification procedure to generate tested extracts (A1-A6). Hippocampal neurons were cultured in the presence of FBS (5%) for 24 h, the starved until treated with indicated extracts at DIV3. (b) Representative images of hippocampal neurons (DIV3) treated for 24 h with control vehicle (DMSO), or indicated extracts (A1-A6) purified from lion's mane mushroom. Neurons were then fixed and processed for immunofluorescence against β-tubulin (green) and imaged using confocal microscopy (nuclear DAPI in blue). Scale bar 20 µm. (c) Longest neurite (axon) length and numbers quantification for each indicated treatments. Data in (c) shows mean ± SEM, $n = 30–60$ neurons in each condition, from 3 neuronal preparations. One-way ANOVA test with Tukey's correction multiple comparison was performed. *p*-value is indicated when significative differences were found.

To examine their effects on the axonal growth cone molecular organization and architecture, extracts A2 to A5, as well as NDPIH (C1) were applied to hippocampal neuronal cultures for 24 h, which were then co-stained using anti-beta-III tubulin and phalloidin-rhodamine (Figure 3). Vehicle treated neurons exhibited classical growth cone architecture with actin localized in peripheral filopodia and tubulin located in the central domain (Figure 3a). A2-, A4-, A5- as well as NDPIH-treated neurons exhibited highly enlarged growth cones, some larger than the cell body itself, and displayed arrays of large filopodia in the peripheral (P) domain, (Figure 3a). Analysis of the area occupied by growth cones relative to DMSO-treated neurons revealed a 2- to 5-fold average increase in size (Figure 3b).

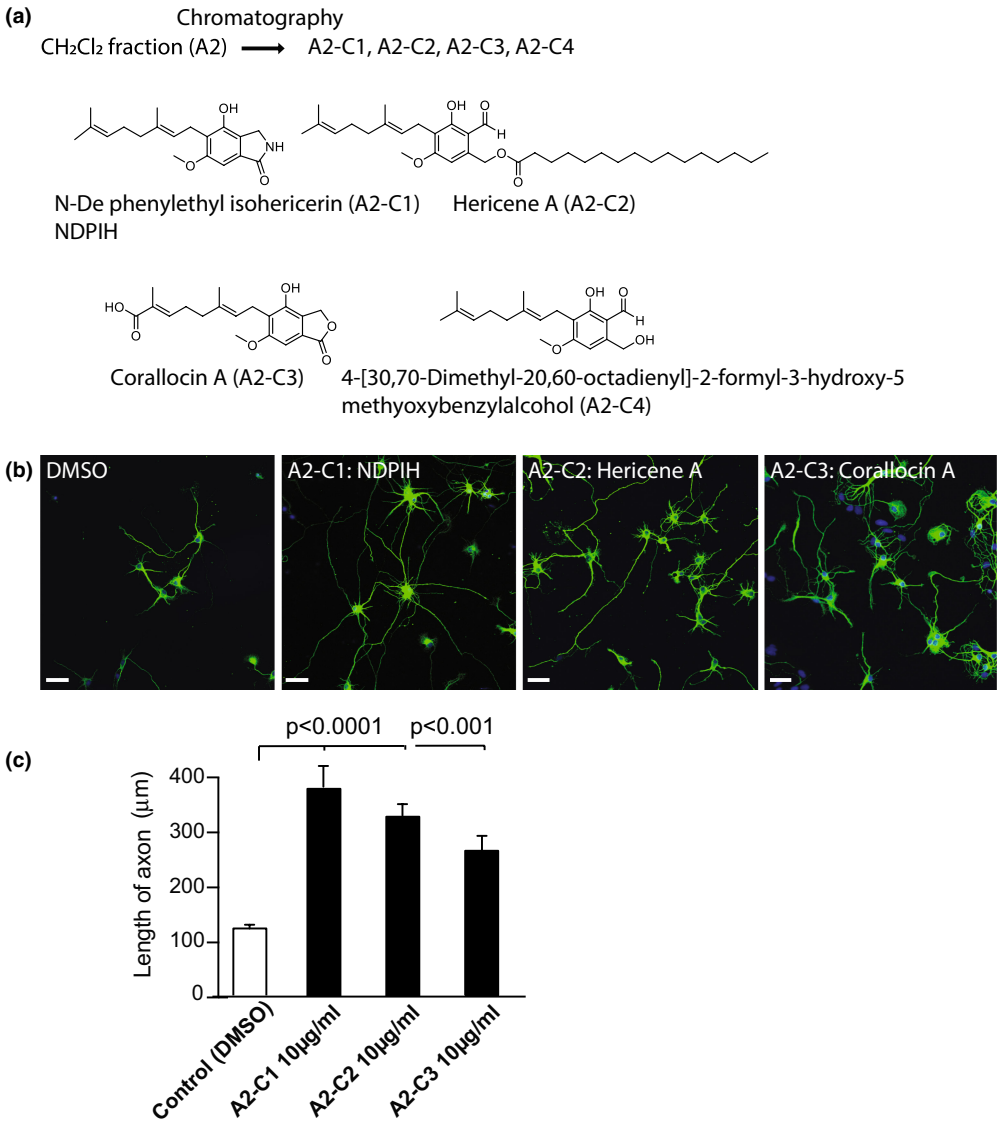

FIGURE 2 A2-derived compounds exert a potent neurotrophic effect in hippocampal neurons. (a) Chemical structures of identified A2-derived compounds. (b) Hippocampal neurons were cultured in the presence of FBS (5%) for 24 h, the starved until treated with indicated extracts at DIV3. (b) Representative images of hippocampal neurons (DIV3) treated for 24 h with control vehicle (DMSO), or indicated extracts (NDPIH, hericene A and Corallocin A). Neurons were then fixed and processed for immunofluorescence against β-tubulin (green) and imaged using confocal microscopy (nuclear DAPI in blue). Scale bar 20 µm. (c) Longest neurite (axon) length quantification for each indicated treatments. Data in (c) shows mean ± SEM, $n = 30–60$ neurons in each condition, from 3 neuronal preparations. One-way ANOVA test with Tukey's correction for multiple comparison was performed. *p*-value is indicated when significative differences were found.

Furthermore, although most microtubules were present in the C-domain of control growth cones, NDPIH treatment promoted formation of microtubule-enriched filopodial structures that extend along the P-domain of growth cones (Figure 3c). The overall cytoskeletal architecture of growth cones was therefore preserved but the size was markedly increased suggestive of high neurotrophic activity. Overall, the *H. erinaceum* extracts were surprisingly active in hippocampal neurons, with hericene A and NDPIH displaying the highest neurotrophic activity.

We investigated whether NDPIH (Figure 4a) could directly promote neurite outgrowth, or whether it was acting via an autocrine mechanism, similar to that suggested for the NGF activity in peripheral neurons (Phan et al., 2014; Zhang et al., 2015). We therefore reduced the number of neurons seeded and omitted any serum during their culture to prevent paracrine effects from neighbor cells (Figure 4b). Under these conditions NDPIH again significantly increased neurite length in a concentration-dependent manner, strongly suggesting a direct BDNF-like neurotrophic action in these central neurons (Figure 4b,c).

To test the hypothesis that NDPIH acted via a BDNF pathway, we incubated the treated neuronal cultures with the BDNF inhibitor ANA-12, a specific TrkB antagonist capable of selectively preventing TrkB auto-phosphorylation by BDNF (Cazorla et al., 2011). Co-incubation the mushroom extract with ANA-12 (0.5 µM) significantly

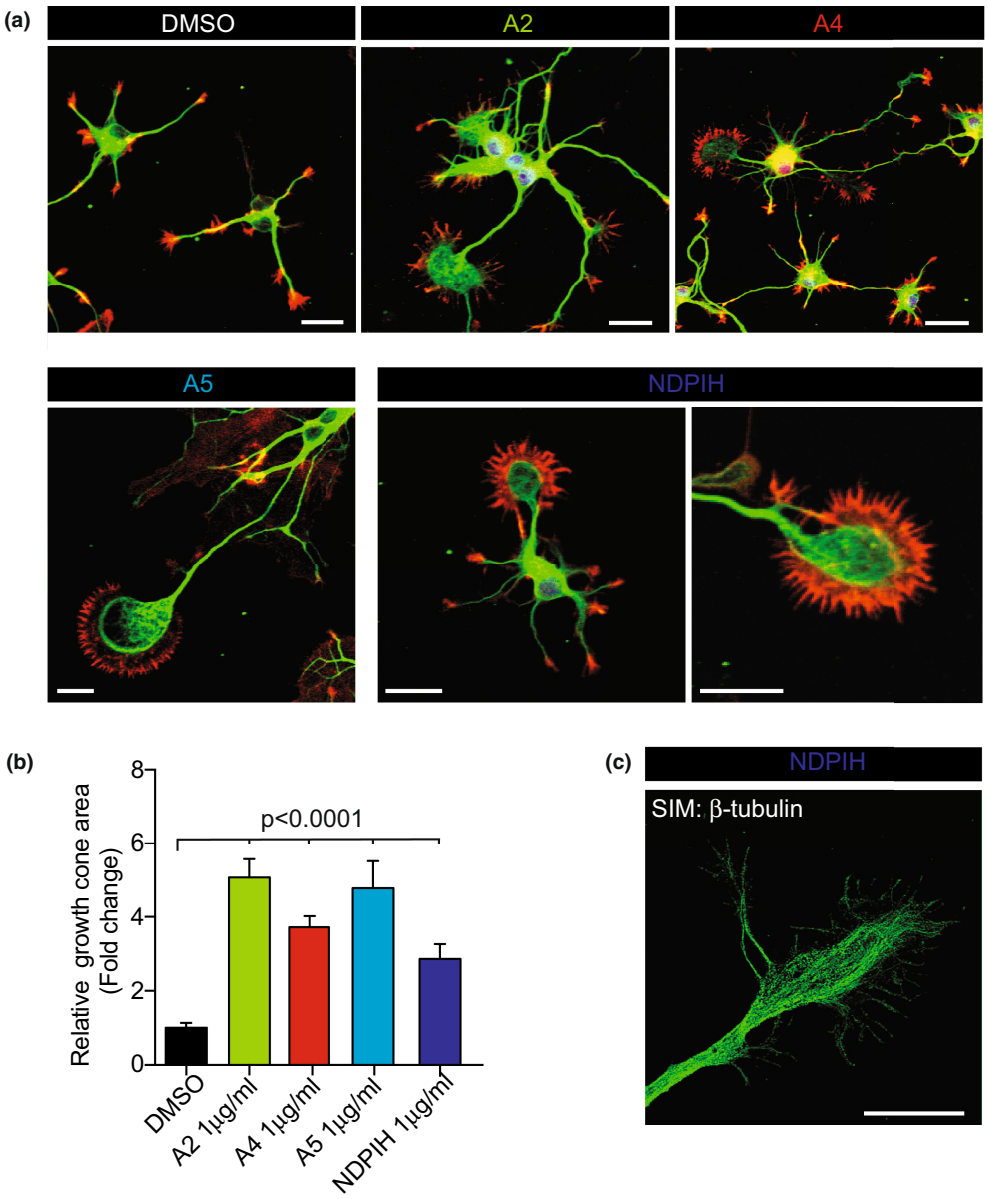

FIGURE 3 Extracts purified from lion's mane mushroom (LMM) exert a neurotrophic effect on growth cone. Hippocampal neurons were cultured in the presence of FBS (5%) for 24 h, the starved until treated with indicated extracts at DIV3. (a) Representative images of hippocampal neurons (DIV3) treated for 24 h with control vehicle (DMSO), or indicated extracts (A2, A4, A5 and NDPIH) purified from lion's mane mushroom. Neurons were then fixed and processed for immunofluorescence against β-tubulin (green) and Actin filaments (red) and imaged using confocal microscopy (nuclear DAPI in blue). (b) Growth cone area quantification for each indicated treatments. Scale bar 50 µm. (c) Representative image of a NDPIH-treated neuron acquired using structure illumination microscopy. Note the classical distribution of microtubules in this enlarged growth cone. Scale bar 50 µm. Data in (b) shows mean ± SEM, $n = 15$ neurons in each condition, from 4 neuronal preparations. One-way ANOVA test with Tukey's correction for multiple comparison was performed. *p*-value is indicated when significative differences were found.

reduced the neurotrophic activity induced by NDPIH but did not completely block the effect (Figure 5a–c). These results suggested that NDPIH-induced neurite outgrowth activities could be partially mediated through the BDNF/TrkB signaling pathway.

To determine whether NDPIH directly activates TrkB, non-transfected or TrkB-transfected HEK-293 T cells were treated either with NDPIH or with an unrelated control extract, or were treated with NDPIH, and/or low concentration of BDNF (1 ng/mL) and/or ANA-12 for 1 h following 5 h of serum starvation. Western blots of cell lysates (Figure S3) were probed with antibodies to total and phosphorylated-TrkA/B, ERK1/2 or Akt (Figure 6a,b). ERK1/2 or Akt are trophic signaling proteins activated down-stream of Trk receptors. ERK1/2 signaling results in neurite outgrowth and synaptogenesis through the phosphorylation of p-CREB, and Akt signaling

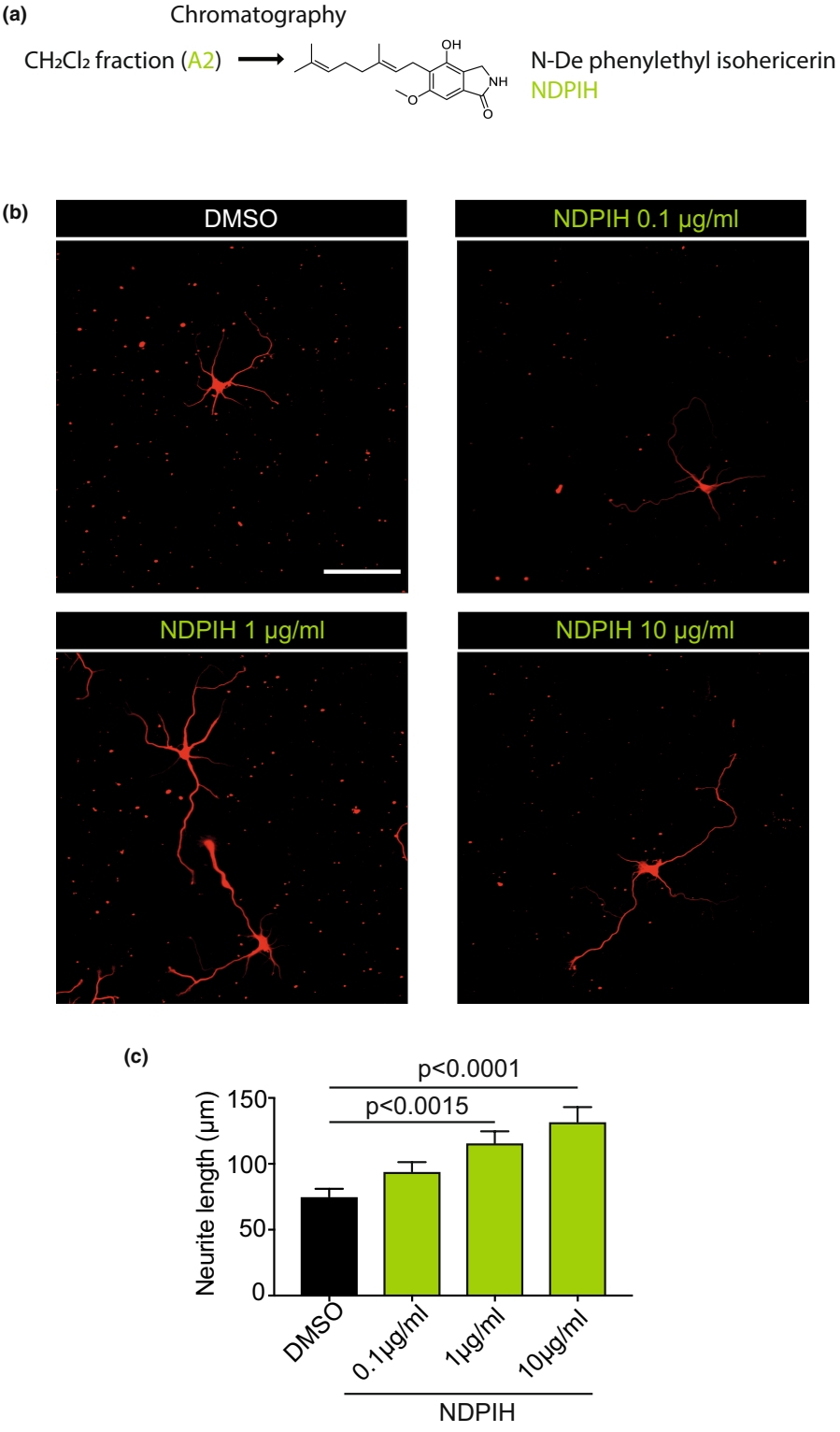

FIGURE 4 NDPIH purified from lion's mane mushroom exerts a dose-dependent neurotrophic effect in hippocampal neurons. (a) Chemical structures of identified A2-derived compound NDPIH. (b) Hippocampal neurons seeded at low density to minimize paracrine effects until DIV2. Cells were then exposed to indicated concentration of purified NDPIH for 24 h, fixed, processed for immunochemistry against β-tubulin (red) and imaged using confocal microscopy. Representative images of hippocampal neurons, treated with control vehicle (DMSO) or indicated concentrations (0.1, 1 or 10 µg/mL) of NDPIH purified from lion's mane mushroom extract A2. Scale bar 100 µm. (c) Axon length quantification for each treatment. Axon was considered as the longest neurite. Data in (c) shows mean ± SEM. $n = 59–102$ neurons in each condition, from 3 neuronal preparations. One-way ANOVA test with Dunnett's correction for multiple comparison was performed. p-value is indicated when significative differences were found, and "ns" is stated when no significant differences were detected.

mediates neuronal survival (Matusica & Coulson, 2014; Mesripour et al., 2016). Surprisingly, NDPIH promoted increased ERK1/2 phosphorylation in un-transfected HEK-293T cells which do not endogenously express TrkB, suggesting a TrkB-independent effect (Figure 6a,c). Cells transfected with TrkB also displayed significantly increased ERK1/2 phosphorylation upon NDPIH treatment, higher to that of transfected cells treated with 1 ng/mL BDNF. However, the levels of phosphorylated TrkB were unchanged in the presence of NDPIH or BDNF (Figure 6b,d). When NDPIH was co-treated with BDNF in TrkB transfected cells, the activation of ERK1/2 signaling was potentiated (Figure 6b,c). Pre-treatment of cells with the TrkB inhibitor ANA-12 did not supress the phosphorylation of ERK1/2

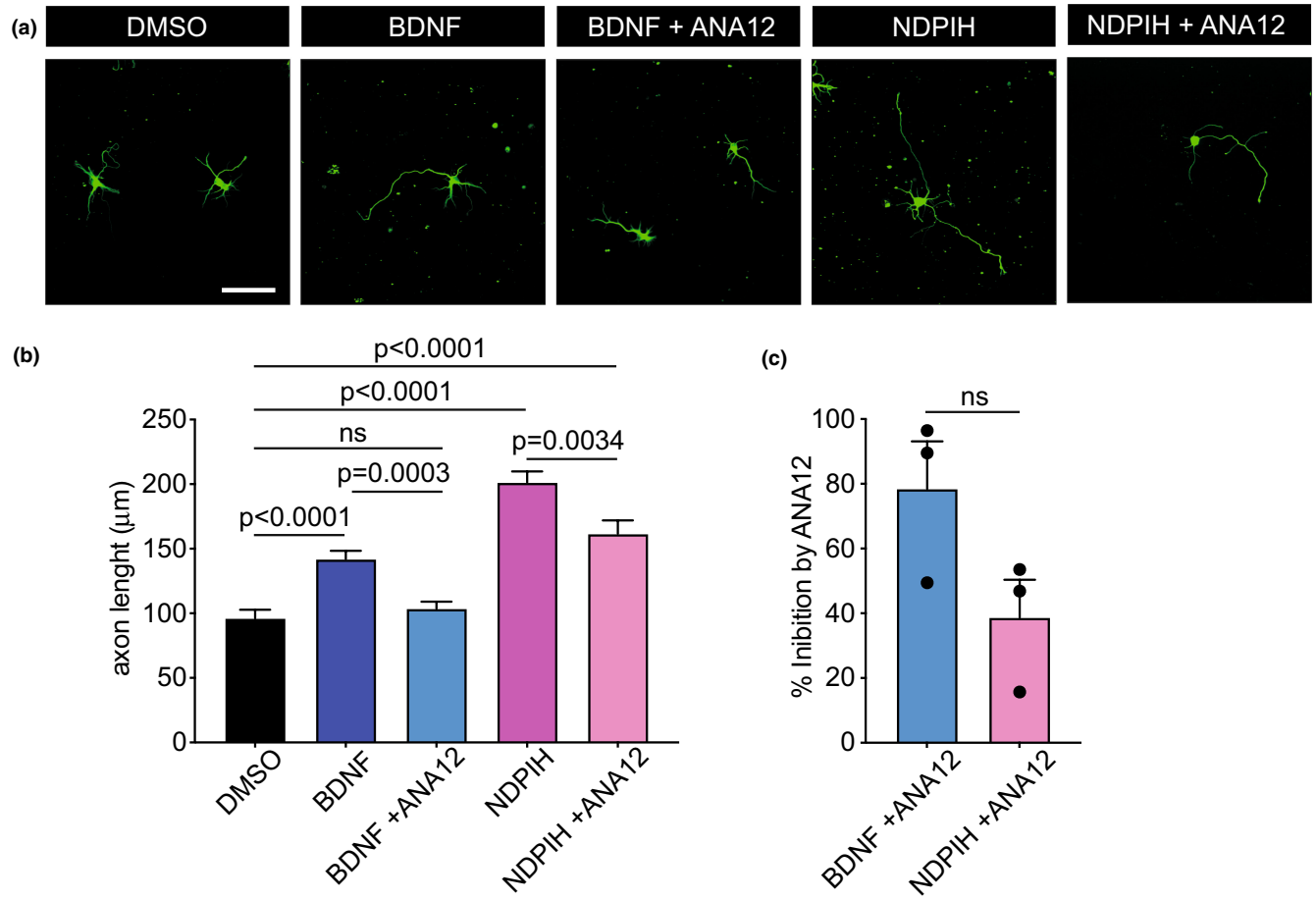

FIGURE 5 NDPIH purified from lion's mane mushroom A2 exerts a BDNF-like neurotrophic effect in hippocampal neurons. (a) Hippocampal neurons seeded at low density to minimize paracrine effects until DIV2. Cells were then exposed to purified NDPIH (10 µg/mL) or BDNF (1 nM) for 24 h in the presence or absence of Trk-B inhibitor ANA-12 (0.5 µM), fixed, processed for immunochemistry against β-tubulin (green) and imaged using confocal microscopy. ANA-12 was added simultaneously to BDNF or NDPIH. Representative images of hippocampal neurons in the indicated conditions. Scale bar 100 µm. (b) Axon length quantification for each treatment. Axon was considered as the longest neurite. (c) Relative inhibition of axon length by ANA-12 on BDNF or NDPIH. Data in (b) and (c) show mean ± SEM. $n = 104–174$ neurons in (b), and $n = 3$ neuronal preparations in (c). One-way ANOVA test with Tukey's correction for multiple comparison was performed in (b), and two-tailed, unpaired Mann–Whitney U test was performed in (c). p-value is indicated when significative differences were found, and "ns" is stated when no significant differences were detected. p-value = 0.2 in (c).

FIGURE 6 NDPIH purified from Lion's mane mushroom A2 potentiates BDNF neurotrophic activity. (a, b) Representative western blot of total protein extracts from HEK-293 T non-transfected (a) or transfected with TrkB (b). The cells were serum-starved for 5 h prior to stimulation with 10 µg/mL of NDPIH mushroom extracts or with a control (unrelated mushroom extract) and/or BDNF (1 ng/mL) for 1 h. ANA-12 (50 µM) was added at time of serum starvation in indicated conditions. Following stimulation, samples were lysed, resolved by SDS-PAGE and immunoblotted with indicated primary antibodies. (c) Combined quantification of pERK1/2 activity from non-transfected or TrkB-transfected cells. (d) Quantification of pTrkB activation in TrkB-transfected cells. Total and phospho-TrkB were immunoblotted following TrkB enrichment from lysates. To quantify densitometry from immunoblots, detected signal was normalized to loading control for each lane (or total TrkB, for phospho-TrkB), prior to calculation of phospho- over total-signal for each protein, expressed as a fold change relative to DMSO (control) treatment. (e) Representative western blot of total protein extracts from HEK-293 T transfected with TrkB. The cells were serum starved, stimulated and processed as in (b) except for BDNF concentration, which was saturating (40 ng/mL). (f) Quantification of densitometry analysis from (e) as above. (g) TrkB+p75^{ICD}-transfected HEK-293 T cells were treated, stimulated and processed as in (a, b). (h) Quantification of densitometry analysis from (g) as above. (i) ATP conversion by the TrkB kinase in response to mushroom extract treatment was measured using the ADP-Glo kinase activity assay system with recombinant TrkB kinase domain. TrkB kinase domain was incubated with NDPIH extract, with control or with staurosporine at the indicated concentrations. Activity is expressed as a percentage of the ATP-conversion by control-treated kinase domain. Data show mean ± SEM, $n = 3$ (c, d, h and i) or $n = 6$ (f) cell culture preparations. One-way ANOVA test with Tukey's correction for multiple comparison was performed. p-value is indicated when significant differences were found, and "ns" is stated when no significant differences were detected.

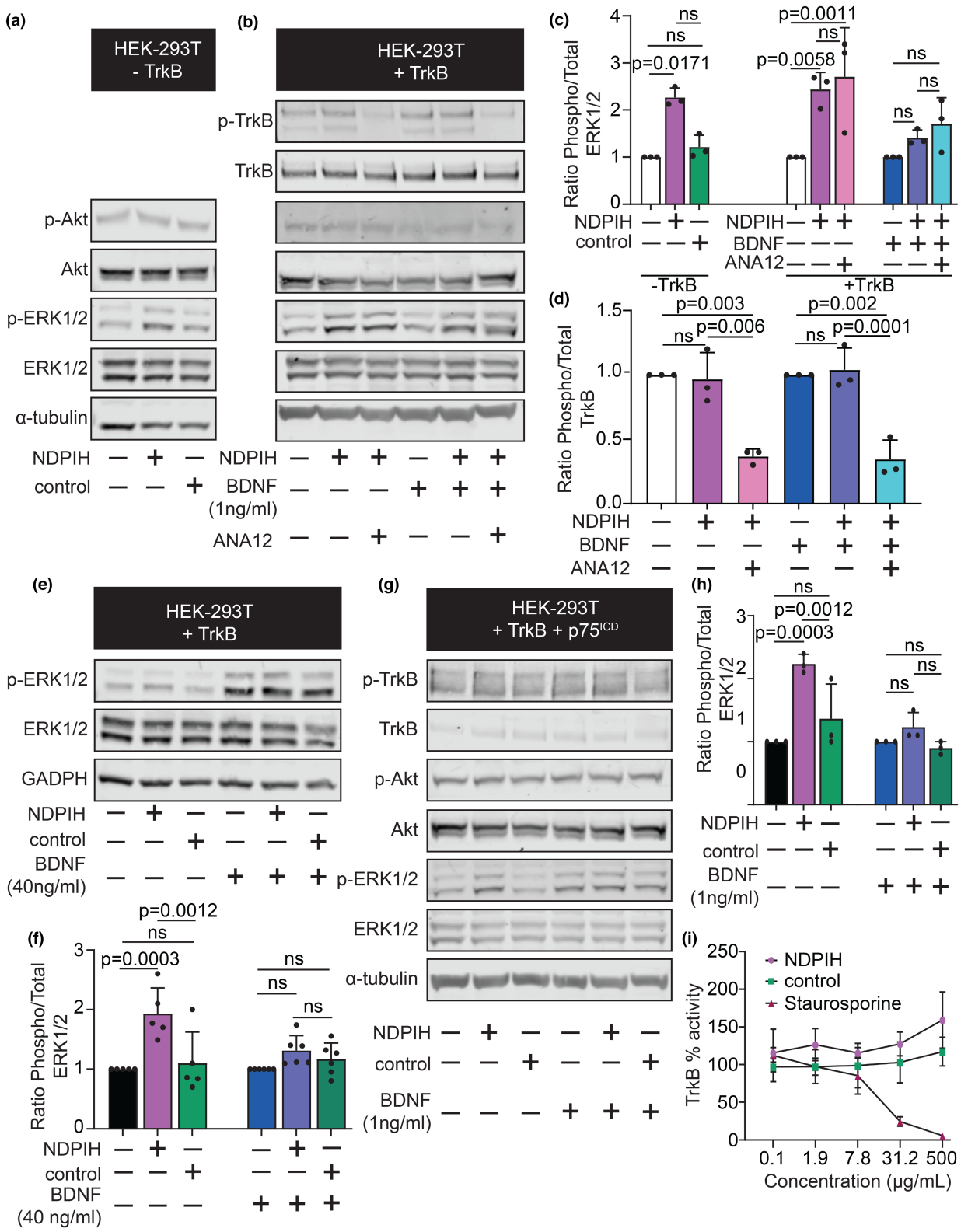

induced by NDPIH alone or combined with BDNF (Figure 6b,c), but decreased the basal phosphorylation of TrkB (Figure 6b,d). When TrkB-transfected cells were treated with saturated concentrations of BDNF (40 ng/mL), the level of ERK1/2 phosphorylation was now higher than that achieved only with NDPIH treatment alone without BDNF (Figure 6e,f). Under these high BDNF concentration, the combination of BDNF and NDPIH treatments did not significantly increase ERK1/2 activity above that of BDNF alone, suggesting that the signal pathway was already maximally activated by this saturating concentration of BDNF (Figure 6e,f).

As TrkB signaling can be modulated by co-expression of the p75 neurotrophin receptor, we asked whether NDPIH acted via

p75-induced modulation. Co-transfection of HEK-293T cells with the p75 intracellular domain to enhance TrkB receptor affinity and signaling, increased ERK1/2 phosphorylation in response to low concentrations of BDNF (Figure 6g,h) as previously shown (Matusica et al., 2013, 2016). Treatment with NDPIH alone also resulted in ERK1/2 phosphorylation, but the combination with BDNF did not further potentiated ERK1/2 signaling influenced by p75 (Figure 6g,h). To further evaluate whether NDPIH has a direct effect on TrkB, we performed in vitro kinase assay using recombinant TrkB (Figure 6i). Increasing concentrations of the mushroom extract NDPIH did not affect TrkB activity (Figure 6i). Our results confirmed that NDPIH does not act through either low- or high-affinity TrkB receptor complexes. Together, these data suggest that NDPIH and BDNF act through distinct but convergent pathways.

Next, we quantified the level of neurotrophins produced, the level of Trk receptor phosphorylation, the phosphorylation of downstream signaling proteins, and the level of synaptogenesis in brain protein extracts (Figure S4, S5) from mice treated with two concentrations (100 mg/kg and 250 mg/kg) of either the crude extract (A1), a single concentration of hericene A (A2-C2), or the nootropic chemical piracetam, a positive control known to enhance rodent cognitive skills (Figure 7a). Mice treated with 250 mg/kg of A1 and hericene A significantly increased the levels of the neurotrophins BDNF, NGF, CNTF and GDNF in comparison to piracetam (Figure 7b–f). Both neurotrophin receptors TrkB and TrkA were also phosphorylated after treatment with A1 and hericene A (Figure 7b,g,h). Mice treated with 250 mg/kg of A1 and 5 mg/kg of hericene A displayed a significantly increased activation of the downstream signaling kinase ERK1/2 and its target CREB (Figure 7b,i,j). SYP is known as a major synaptic protein involved in synapse formation and its level is used to quantify synaptogenesis (Baruch-Eliyahu et al., 2019). Our result also showed that A1 and hericene A increased SYP level in treated mice, compared with the piracetam-treated animals (Figure 7b,k), suggesting that the treatment with either of both extracts resulted in elevated synaptic formation. The neurotrophin BDNF is considered a bona fide neurotrophic factor, whose role in enhancing memory function by promoting neuronal survival and differentiation in brain in vivo has been demonstrated (Miranda et al., 2019). Thus, we further examined whether A1 and hericene A increased the levels of BDNF in brain mice regions by immunostaining assays (Figure 8a). Our results showed that oral administration of either A1 and hericene A resulted in increased levels of BDNF both in the dentate gyrus (DG) of the hippocampus (Figure 8b) and in cortical regions (Figure 8c). Overall, our results in vitro and in vivo suggest a positive pan-neurotropic action of extracts derived from *H. erinaceum*.

We then evaluated the effect of both the A1 crude extract and hericene A on short-term memory acquisition, which was assayed using the novel object recognition test (NORT) and the Y-maze test (Figure 9a). In the NORT paradigm of memory test (Figure S6), our control treatment failed to show evident short-term/working memory performance (Figure 9b). However, the highest administration of A1 (250 mg/kg) and hericene A displayed significantly enhanced interaction with the novel object compared with the control (normal, vehicle) group (Figure 9b), without affecting the mean velocity or the total distance traveled of the animals (Figure S7). The same cohort of mice were also tested in the Y-maze test (Figure S8). The nootropic chemical piracetam group exhibited a significant increase in alternation behavior, compared with the control (vehicle) group. In this case, both concentrations of A1-treated groups (100 mg/kg and 250 mg/kg) and the hericene A group did exhibit significant increments in spontaneous alternation of the behavior (Figure 9c,d), without altering the mean velocity or the total distance traveled of the animals (Figure S9), suggesting improvements in memory acquisition. Together these findings demonstrate that the *H. erinaceus* extracts have an enhancing effect on spatial memory and suggest that this effect stems from a pan-neurotrophic activity in the mouse brain, via the enhanced expression of neurotrophins and downstream ERK1/2 signaling.

4 | DISCUSSION

Here we demonstrate that crude and purified extracts of the nootropic mushroom *H. erinaceus* have BDNF-like neurotrophic activity both in cultured hippocampal neurons and in paradigm models of learning in vivo, leading to marked neurite outgrowth and improved memory. *H. erinaceum* mushroom characteristically contains aromatic and diterpene skeletons as active components, providing a large source of structurally related terpenoids, such as erinacines, hericenones, hericerins, hericenes, hericenols, and erinacerins that can have bioactivity. In fact, *H. erinaceus* contains 20 out of all 24 known diterpenoids (Friedman, 2015). We purified four aromatic compounds from the CH_2Cl_2 fraction (C1 to C4) with prenyl side chains: NDPIH, hericene A, corallocin A, and 4-[3′,7′-dimethyl-2′,6′-octadienyl]-2-formyl-3-hydroxy-5-methyoxybenzylalcohol and found that they have the ability to elicit strong survival and neurotrophic responses on neuronal cultures in the absence of (and thereby replacing) serum supplementation. Previously, corallocin A (C3) was shown to induce NGF and BDNF expression in astrocytes (Wittstein et al., 2016). Similarly, *Hericenones* aromatic compounds stimulate NGF secretion from PC12 cells (Phan et al., 2014) and erinacines diterpene compounds stimulate NGF synthesis in other in vitro and in vivo systems (Li et al., 2020; Tsai-Teng et al., 2016).

Neurotrophins also regulate the plasticity and growth of axons within the adult central and peripheral nervous system (Guthrie, 2007). However, the expression of many neurotrophic factors is greatly reduced within the adult CNS. Exogenous application of these growth-permissive neurotrophic factors has therapeutic potential through creation of favorable environments after nerve injury (Keefe et al., 2017). Supplementation of NGF and BDNF have been used to promote survival and axonal regrowth

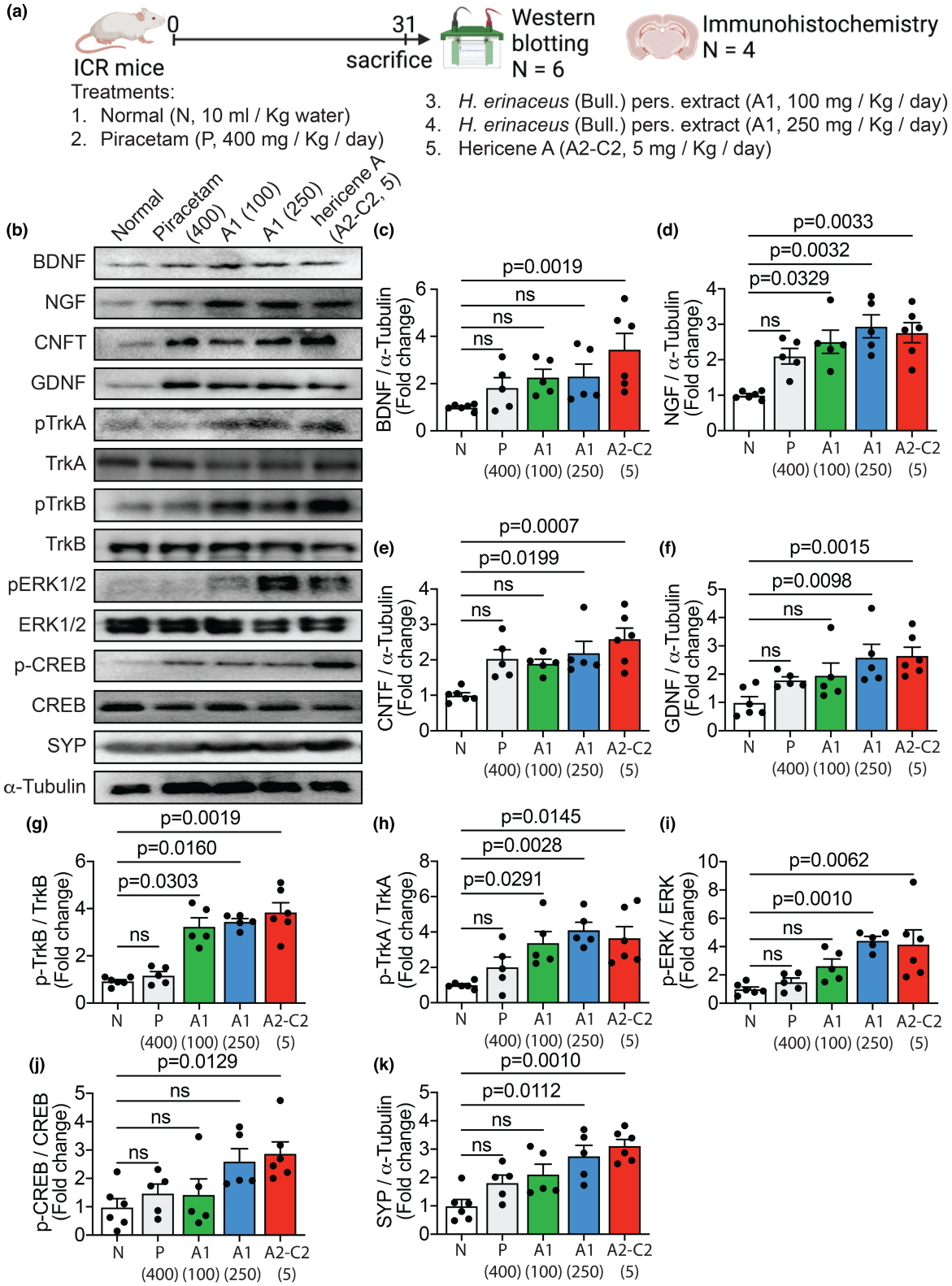

FIGURE 7 Lion's mane mushroom A1 and A2-derived hericene dietary treatment increase neurotrophic signaling in vivo. (a) Scheme of the experimental design. Mice were feeded with either A1 (100 or 250 mg/kg), hericene A (A2-C2, 5 mg/kg), piracetam (PC, 400 mg/kg) or vehicle control during 31 days, before their brains (whole) were collected and the tissue was lysed and prepared for western blot analysis. (b) Representative western blots of anti-BDNF, NGF, CNTF, p-TrkA, TrkA, p-TrkB, TrkB, p-ERK, ERK, p-CREB, CREB, SYP and α-Tubulin. α-Tubulin was used as loading control. (c–k) Quantification of the relative protein expression levels of BDNF (c), NGF (d), CNTF (e), GDNF (f), p-TrkB (g), p-TrkA (h), p-ERK (i) and p-CREB (j), SYP (k). All data are expressed as the mean ± SEM, $n = 5–6$ whole brain lysates. One-way ANOVA followed by Tukey's post hoc test was performed. *p*-value is indicated when significant differences were found, and "ns" is stated when no significant differences were detected.

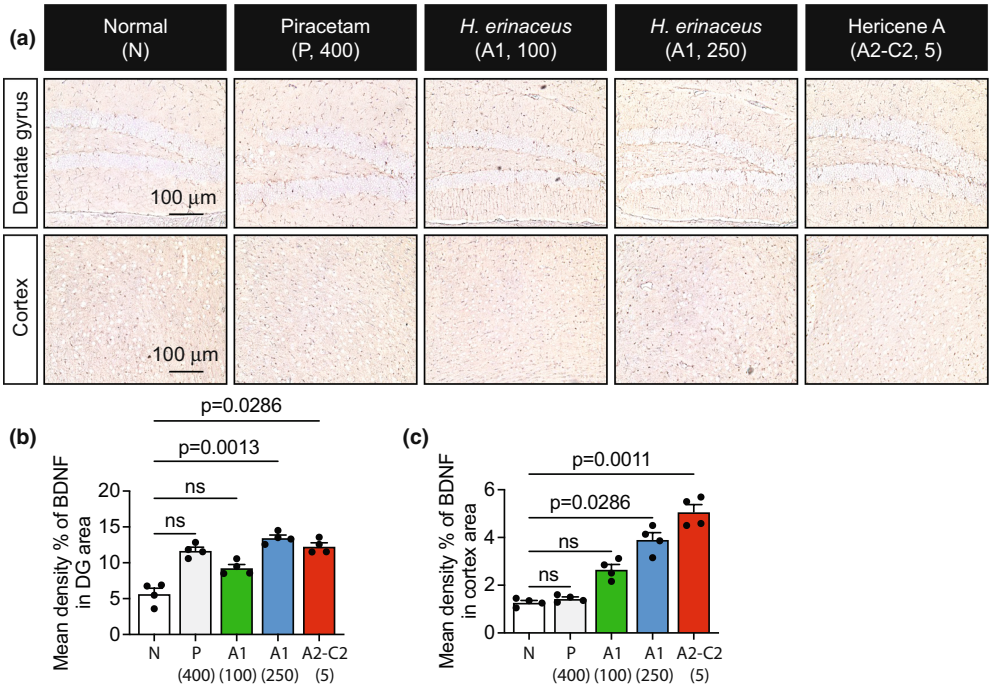

FIGURE 8 Lion's mane mushroom A1 and A2-derived hericene A dietary treatment increase BDNF levels in brain. Mice were treated with either A1 (100 or 250 mg/kg), hericene A (A2-C2, 5 mg/kg), piracetam (PC, 400 mg/kg) or vehicle control during 31 days, before their brains were collected and prepared for immunohistochemistry analysis. (a) The obtained brain sections were immunostained using anti-BDNF antibody. The images were photographed at 10× magnification. The optical density of BDNF immunoreactivity was analyzed in the dentate gyrus (DG) (b) and in the cortex region (c). All data are expressed as the mean ± SEM, $n = 4$ brains. One-way ANOVA followed by Tukey's post hoc test was performed. *p*-value is indicated when significant differences were found, and "ns" is stated when no significant differences were detected.

of injured neurons after spinal cord injury (Harvey et al., 2015). In this context, in vitro studies using total extract of *H. erinaceus* reported regenerative capabilities on peripheral neurons after laser microdissection (Ustun & Ayhan, 2019). This opens the door to additional studies using specific and more potent derivatives from *H. erinaceus* to identify their potential therapeutical action during axon regeneration.

To the best of our knowledge, our study is the first to identify a pro-BDNF signaling-enhancing activity for *H. erinaceus* and to identify hericene A as an active component for this neurotrophic function in vitro and in vivo. Our study reveals that hericene A enhances recognition memory at concentrations as low as 5 mg/kg/day. The medicinal mushroom *H. erinaceus* has long been known for its neurotrophic activity on the peripheral nervous system through promotion of NGF synthesis (Haure-Mirande et al., 2017; Lai et al., 2013; Raman et al., 2015; Ustun & Ayhan, 2019). Several compounds extracted from *H. erinaceus* have been shown to protect from aging-dependent cognitive decline in wild-type (Brandalise et al., 2017; Rossi et al., 2018) and in Alzheimer's disease mouse models (Mori et al., 2011; Tsai-Teng et al., 2016) suggesting a yet to be defined activity on the CNS. A recent study has determined that erinacine A and hericenones C and D were capable of slowing cognitive decline in a model of frailty (Ratto et al., 2019). The neuroprotective effects were attributed to the ability of these molecules to elicit NGF (Mori et al., 2009) and BDNF synthesis (Chiu et al., 2018). In agreement with previous studies, we identified that polysaccharides isolated from *H. erinaceus* extracts also exert a neurotrophic activity. The effects of *H. erinaceus* on recognition memory were previously shown and hypothesized to stem from promoting neurogenesis (Brandalise et al., 2017; Rossi et al., 2018).

Our study demonstrates that hericene A promotes neuritogenesis and that this effect can be achieved at very low concentration both in vitro and in vivo. The highest contents of hericene A were detected in *H. erinaceus* A1 extract, compared with the other species. To increase the production of these compounds, it might be possible to engineer new methods to improve selection of specific *H. erinaceus* strains based on their ability to produce larger quantities of hericene A derivatives. We should also provide an additional step towards hericene A-enriched *H. erinaceus*, marker compound-based standardization for sustainable use of dietary supplements and medicinal products from *H. erinaceus*. Based on our results, we suggest that the administration of hericene A from *H. erinaceus* may be useful to ameliorate brain function and disorder-related pathologies in in vivo neurodegenerative disease models. Although further studies are required to test this hypothesis, our report represents the first step on exploring the potential nootrophic benefits from hericene A compounds isolated from the mushroom *H. erinaceus*.

Since the discovery of the first neurotrophin, NGF, more than 70 years ago, countless studies have demonstrated their ability to

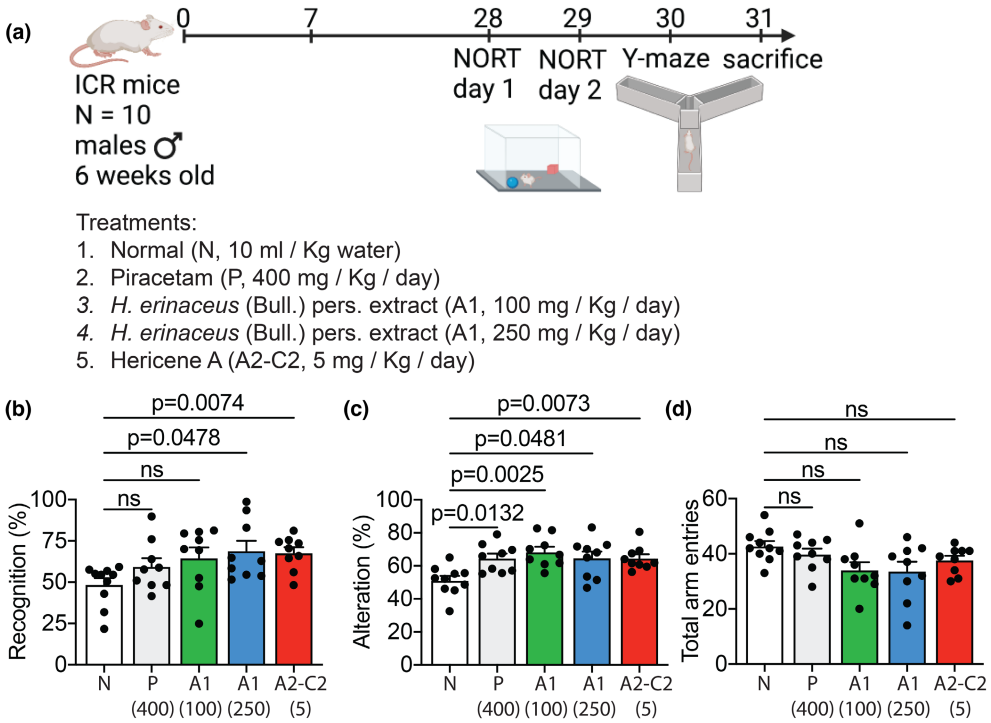

FIGURE 9 Lion's mane mushroom A1 and A2-derived hericene dietary treatment improve recognition memory in mice. (a) Scheme of the experimental design. Mice were treated either with A1 (100 or 250 mg/kg), hericene A (A2-C2, 5 mg/kg), piracetam (PC, 400 mg/kg) or vehicle control (Normal) during 31 days. After testing, mice were sacrificed. (b–d) Quantifications of the behavioral test performed. The NORT test measures the portion of time spent exploring novel object, and expressed as the % of time spent exploring from the total. The NORT test was performed at day 28 and at day 29 (b). The Y-maze test measures the spontaneous alternation of number of arm entries, and is expressed as the % of alternation (c) and as the total arm entries (d). All data are expressed as the mean ± SEM, $n = 9–10$ animals. One-way ANOVA followed by Dunnett's T3 post hoc test was performed. *p*-value is indicated when significant differences were found, and "ns" is stated when no significant differences were detected.

promote neurite regeneration, prevent or reverse neuronal degeneration and enhance synaptic plasticity. Neurotrophins have attracted the attention of the scientific community in the view to implement therapeutic strategies for the treatment of a number of neurological disorders (Chao et al., 2006). Unfortunately, their actual therapeutic applications have been limited and the potential use of their beneficial effects remain to be exploited (Nagahara & Tuszynski, 2011). Neurotrophins, for example, have poor oral bioavailability, and very low stability in serum, with half-lives in the order of minutes (Zhang et al., 2014) as well as minimal BBB permeability and restricted diffusion within brain parenchyma (Pardridge, 2002). In addition, their receptor signaling networks can confer undesired off-target effects such as pain, spasticity and even neurodegeneration (Bergmann et al., 1998; Constandil et al., 2011; Dyck et al., 1997; Endo et al., 2009; Fahnestock et al., 2001; Fouad et al., 2013; Mufson et al., 2012). As a consequence, alternative strategies to increase neurotrophin levels, improve their pharmacokinetic limitations or target specific receptors have been developed (Longo & Massa, 2013). Identification of bioactive compounds derived from natural products with neurotrophic activities also provide new hope in the development of sustainable therapeutical interventions. Hericerin derivative are therefore attractive compounds for their ability to promote a pan-neurotrophic effect with converging ERK1/2 downstream signaling pathway and for their ability to promote the expression of neurotrophins. Further work will be needed to find the direct target of Hericerin capable of mediating such a potent pan-neurotrophic activity and establish whether this novel pathway can be harnessed to improve memory performance and for slowing down the cognitive decline associated with ageing and neurodegenerative diseases.

AUTHOR CONTRIBUTIONS

F.A.M., R.M-M., Y.Ch., K.L., S.Y.K., D.H.L. and J.K.L. conceptualized of the project. R.M-M. and Y.Ch., designed, performed, and analyzed the experiments using neuronal cultures. D.H.L. J.K.L. sourced the lion mane mushroom and S.B.K purified all the extracts under the supervision of K.L. J.N.C performed the experiments using cell lines under the supervision of E.J.C. J.N.C., E.J.C. and R.M-M. analyzed the experiments using cell lines. S-M.H. and Z.K. performed the animal experiments under the supervision of S.Y.K. S-M.H., Z.K. and R.M-M analyzed the animal experiments. All authors discussed and interpreted the data. F.A.M., R.M-M., wrote a first draft of the manuscript with the help of all co-authors. R.M-M., Y.Ch., J.N.C., S-M-H., R.A.G., M.K.L., S.Y.K. and F.A.M. edited the final version of the manuscript. D.H.L., J.K.L., S.Y.K. and F.A.M. acquired the required funding.

ACKNOWLEDGMENTS

This work was supported by an NHMRC Senior Research Fellowship (GNT1155794), Australian Research Council LIEF Grant LE130100078 and CNG-Bio grant Funding to F.A.M. R.M.M. was funded by the Clem and Jones Foundation, the State Government of Queensland, and NHMRC Boosting Dementia Research Initiative. M.K.L was funded by Medical Research Centre program (2017R1A5A2015541) and the National Research Foundation of Korea. Open access publishing facilitated by The University of Queensland, as part of the Wiley - The University of Queensland agreement via the Council of Australian University Librarians. Open access publishing facilitated by The University of Queensland, as part of the Wiley - The University of Queensland agreement via the Council of Australian University Librarians.

All experiments were conducted in compliance with the ARRIVE guidelines.

CONFLICT OF INTEREST STATEMENT

This work was supported by the company CNG-Bio inc. Frédéric A. Meunier is a former editor of the Journal of Neurochemistry.

DATA AVAILABILITY STATEMENT

A preprint of this article was posted on BioRxiv on 28th August 2020: https://www.biorxiv.org/content/10.1101/2020.08.28.271676v1.

ORCID

Ramón Martínez-Mármol https://orcid.org/0000-0003-0929-8627
Rachel S. Gormal https://orcid.org/0000-0003-1604-0253
Elizabeth J. Coulson https://orcid.org/0000-0003-3783-6197
Frédéric A. Meunier https://orcid.org/0000-0001-6400-1107

REFERENCES

Allen, S. J., Watson, J. J., & Dawbarn, D. (2011). The neurotrophins and their role in Alzheimer's disease. *Current Neuropharmacology*, *9*, 559–573.

Bae, H. J., Kim, J., Kim, J., Goo, N., Cai, M., Cho, K., Jung, S. Y., Kwon, H., Kim, D. H., Jang, D. S., & Ryu, J. H. (2020). The effect of maslinic acid on cognitive dysfunction induced by cholinergic blockade in mice. *Br J Pharmacol*, *177*, 3197–3209.

Baruch-Eliyahu, N., Rud, V., Braiman, A., & Priel, E. (2019). Telomerase increasing compound protects hippocampal neurons from amyloid beta toxicity by enhancing the expression of neurotrophins and plasticity related genes. *Scientific Reports*, *9*, 18118.

Bergmann, I., Reiter, R., Toyka, K. V., & Koltzenburg, M. (1998). Nerve growth factor evokes hyperalgesia in mice lacking the low-affinity neurotrophin receptor p75. *Neuroscience Letters*, *255*, 87–90.

Brandalise, F., Cesaroni, V., Gregori, A., Repetti, M., Romano, C., Orrù, G., Botta, L., Girometta, C., Guglielminetti, M. L., Savino, E., & Rossi, P. (2017). Dietary supplementation of *Hericium erinaceus* increases mossy fiber-CA3 hippocampal neurotransmission and recognition memory in wild-type mice. *Evidence-Based Complementary and Alternative Medicine*, *2017*, 3864340–3864313.

Cazorla, M., Premont, J., Mann, A., Girard, N., Kellendonk, C., & Rognan, D. (2011). Identification of a low-molecular weight TrkB antagonist with anxiolytic and antidepressant activity in mice. *The Journal of Clinical Investigation*, *121*, 1846–1857.

Chan, S. J., Love, C., Spector, M., Cool, S. M., Nurcombe, V., & Lo, E. H. (2017). Endogenous regeneration: Engineering growth factors for stroke. *Neurochemistry International*, *107*, 57–65.

Chao, M. V. (2003). Neurotrophins and their receptors: A convergence point for many signalling pathways. *Nature Reviews. Neuroscience*, *4*, 299–309.

Chao, M. V., Rajagopal, R., & Lee, F. S. (2006). Neurotrophin signalling in health and disease. *Clinical Science (London, England)*, *110*, 167–173.

Chiu, C. H., Chyau, C. C., Chen, C. C., Lee, L. Y., Chen, W. P., Liu, J. L., Lin, W. H., & Mong, M. C. (2018). Erinacine A-enriched *Hericium erinaceus* mycelium produces antidepressant-like effects through modulating BDNF/PI3K/Akt/GSK-3beta signaling in mice. *International Journal of Molecular Sciences*, *19*, 341.

Constandil, L., Aguilera, R., Goich, M., Hernandez, A., Alvarez, P., Infante, C., & Pelissier, T. (2011). Involvement of spinal cord BDNF in the generation and maintenance of chronic neuropathic pain in rats. *Brain Research Bulletin*, *86*, 454–459.

Dyck, P. J., Peroutka, S., Rask, C., Burton, E., Baker, M. K., Lehman, K. A., Gillen, D. A., Hokanson, J. L., & O'Brien, P. C. (1997). Intradermal recombinant human nerve growth factor induces pressure allodynia and lowered heat-pain threshold in humans. *Neurology*, *48*, 501–505.

Endo, T., Ajiki, T., Inoue, H., Kikuchi, M., Yashiro, T., Nakama, S., Hoshino, Y., Murakami, T., & Kobayashi, E. (2009). Early exercise in spinal cord injured rats induces allodynia through TrkB signaling. *Biochemical and Biophysical Research Communications*, *381*, 339–344.

Fahnestock, M., Michalski, B., Xu, B., & Coughlin, M. D. (2001). The precursor pro-nerve growth factor is the predominant form of nerve growth factor in brain and is increased in Alzheimer's disease. *Molecular and Cellular Neurosciences*, *18*, 210–220.

Fouad, K., Bennett, D. J., Vavrek, R., & Blesch, A. (2013). Long-term viral brain-derived neurotrophic factor delivery promotes spasticity in rats with a cervical spinal cord hemisection. *Frontiers in Neurology*, *4*, 187.

Friedman, M. (2015). Chemistry, nutrition, and health-promoting properties of *Hericium erinaceus* (Lion's mane) mushroom fruiting bodies and mycelia and their bioactive compounds. *Journal of Agricultural and Food Chemistry*, *63*, 7108–7123.

Guthrie, S. (2007). Neurotrophic factors: Are they axon guidance molecules? *Advances in Experimental Medicine and Biology*, *621*, 81–94.

Harvey, A. R., Lovett, S. J., Majda, B. T., Yoon, J. H., Wheeler, L. P., & Hodgetts, S. I. (2015). Neurotrophic factors for spinal cord repair: Which, where, how and when to apply, and for what period of time? *Brain Research*, *1619*, 36–71.

Haure-Mirande, J. V., Audrain, M., Fanutza, T., Kim, S. H., Klein, W. L., Glabe, C., Readhead, B., Dudley, J. T., Blitzer, R. D., Wang, M., Zhang, B., Schadt, E. E., Gandy, S., & Ehrlich, M. E. (2017). Deficiency of TYROBP, an adapter protein for TREM2 and CR3 receptors, is neuroprotective in a mouse model of early Alzheimer's pathology. *Acta Neuropathologica*, *134*, 769–788.

Hazekawa, M., Kataoka, A., Hayakawa, K., Uchimasu, T., Furuta, R., Irie, K., Akitake, Y., Yoshida, M., Fujioka, T., Egashira, N., Oishi, R., Mishima, K., Mishima, K., Uchida, T., Iwasaki, K., & Fujiwara, M. (2010). Neuroprotective effect of repeated treatment with *Hericium erinaceum* in mice subjected to middle cerebral artery occlusion. *Journal of Health Science*, *56*, 296–303.

Hu, J. H., Li, I. C., Lin, T. W., Chen, W. P., Lee, L. Y., Chen, C. C., & Kuo, C. F. (2019). Absolute bioavailability, tissue distribution, and excretion of erinacine S in *Hericium erinaceus* mycelia. *Molecules*, *24*, 1624.

Ip, N. Y., Li, Y., Yancopoulos, G. D., & Lindsay, R. M. (1993). Cultured hippocampal neurons show responses to BDNF, NT-3, and NT-4, but not NGF. *The Journal of Neuroscience*, *13*, 3394–3405.

Joensuu, M., Martinez-Marmol, R., Padmanabhan, P., et al. (2017). Visualizing endocytic recycling and trafficking in live neurons by subdiffractional tracking of internalized molecules. *Nature Protocols*, *12*, 2590–2622.

Joensuu, M., Padmanabhan, P., Durisic, N., Bademosi, A. T. D., Cooper-Williams, E., Morrow, I. C., Harper, C. B., Jung, W. R., Parton, R. G., Goodhill, G. J., Papadopulos, A., & Meunier, F. A. (2016). Subdiffractional tracking of internalized molecules reveals heterogeneous motion states of synaptic vesicles. *The Journal of Cell Biology*, *215*, 277–292.

Kaplan, D. R., & Miller, F. D. (2000). Neurotrophin signal transduction in the nervous system. *Current Opinion in Neurobiology*, *10*, 381–391.

Kawagishi, H., Shimada, A., Hosokawa, S., Mori, H., Sakamoto, H., Ishiguro, Y., Sakemi, S., Bordner, J., Kojima, N., & Furukawa, S. (1996). Erinacines E, F, and G, stimulators of nerve growth factor (NGF)-synthesis, from the mycelia of *Hericium erinaceum*. *Tetrahedron Letters*, *37*, 7399–7402.

Kawagishi, H., & Zhuang, C. (2008). Compounds for dementia from *Hericium erinaceum*. *Drug Future*, *33*, 149–155.

Keefe, K. M., Sheikh, I. S., & Smith, G. M. (2017). Targeting neurotrophins to specific populations of neurons: NGF, BDNF, and NT-3 and their relevance for treatment of spinal cord injury. *International Journal of Molecular Sciences*, *18*, 548.

Kim, S. P., Nam, S. H., & Friedman, M. (2013). *Hericium erinaceus* (Lion's mane) mushroom extracts inhibit metastasis of cancer cells to the lung in CT-26 colon cancer-tansplanted mice. *Journal of Agricultural and Food Chemistry*, *61*, 4898–4904.

Lai, P. L., Naidu, M., Sabaratnam, V., Wong, K. H., David, R. P., Kuppusamy, U. R., Abdullah, N., & Malek, S. N. (2013). Neurotrophic properties of the Lion's mane medicinal mushroom, *Hericium erinaceus* (higher basidiomycetes) from Malaysia. *International Journal of Medicinal Mushrooms*, *15*, 539–554.

Li, I. C., Chang, H. H., Lin, C. H., Chen, W. P., Lu, T. H., Lee, L. Y., Chen, Y. W., Chen, Y. P., Chen, C. C., & Lin, D. P. C. (2020). Prevention of early Alzheimer's disease by erinacine A-enriched *Hericium erinaceus* mycelia pilot double-blind placebo-controlled study. *Frontiers in Aging Neuroscience*, *12*, 155.

Li, W., Zhou, W., Kim, E. J., Shim, S. H., Kang, H. K., & Kim, Y. H. (2015). Isolation and identification of aromatic compounds in Lion's mane mushroom and their anticancer activities. *Food Chemistry*, *170*, 336–342.

Longo, F. M., & Massa, S. M. (2013). Small-molecule modulation of neurotrophin receptors: A strategy for the treatment of neurological disease. *Nature Reviews. Drug Discovery*, *12*, 507–525.

Matusica, D., Alfonsi, F., Turner, B. J., Butler, T. J., Shepheard, S. R., Rogers, M. L., Skeldal, S., Underwood, C. K., Mangelsdorf, M., & Coulson, E. J. (2016). Inhibition of motor neuron death *in vitro* and in vivo by a p75 neurotrophin receptor intracellular domain fragment. *Journal of Cell Science*, *129*, 517–530.

Matusica, D., & Coulson, E. J. (2014). Local versus long-range neurotrophin receptor signalling: Endosomes are not just carriers for axonal transport. *Seminars in Cell & Developmental Biology*, *31*, 57–63.

Matusica, D., Skeldal, S., Sykes, A. M., Palstra, N., Sharma, A., & Coulson, E. J. (2013). An intracellular domain fragment of the p75 neurotrophin receptor (p75(NTR)) enhances tropomyosin receptor kinase a (TrkA) receptor function. *The Journal of Biological Chemistry*, *288*, 11144–11154.

Mesripour, A., Moghimi, F., & Rafieian-Kopaie, M. (2016). The effect of *Cinnamomum zeylanicum* bark water extract on memory performance in alloxan-induced diabetic mice. *Research in Pharmaceutical Sciences*, *11*, 318–323.

Minichiello, L., Korte, M., Wolfer, D., Kühn, R., Unsicker, K., Cestari, V., Rossi-Arnaud, C., Lipp, H. P., Bonhoeffer, T., & Klein, R. (1999). Essential role for TrkB receptors in hippocampus-mediated learning. *Neuron*, *24*, 401–414.

Miranda, M., Morici, J. F., Zanoni, M. B., & Bekinschtein, P. (2019). Brain-derived neurotrophic factor: A key molecule for memory in the healthy and the pathological brain. *Frontiers in Cellular Neuroscience*, *13*, 363.

Mori, K., Inatomi, S., Ouchi, K., Azumi, Y., & Tuchida, T. (2009). Improving effects of the mushroom Yamabushitake (*Hericium erinaceus*) on mild cognitive impairment: A double-blind placebo-controlled clinical trial. *Phytotherapy Research*, *23*, 367–372.

Mori, K., Obara, Y., Moriya, T., Inatomi, S., & Nakahata, N. (2011). Effects of *Hericium erinaceus* on amyloid beta(25-35) peptide-induced learning and memory deficits in mice. *Biomedical Research*, *32*, 67–72.

Mufson, E. J., He, B., Nadeem, M., Perez, S. E., Counts, S. E., Leurgans, S., Fritz, J., Lah, J., Ginsberg, S. D., Wuu, J., & Scheff, S. W. (2012). Hippocampal proNGF signaling pathways and beta-amyloid levels in mild cognitive impairment and Alzheimer disease. *Journal of Neuropathology and Experimental Neurology*, *71*, 1018–1029.

Nagahara, A. H., & Tuszynski, M. H. (2011). Potential therapeutic uses of BDNF in neurological and psychiatric disorders. *Nature Reviews. Drug Discovery*, *10*, 209–219.

Pardridge, W. M. (2002). Neurotrophins, neuroprotection and the blood-brain barrier. *Current Opinion in Investigational Drugs*, *3*, 1753–1757.

Phan, C. W., Lee, G. S., Hong, S. L., Wong, Y. T., Brkljaca, R., Urban, S., Abd Malek, S. N., & Sabaratnam, V. (2014). *Hericium erinaceus* (bull.: Fr) Pers. cultivated under tropical conditions: Isolation of hericenones and demonstration of NGF-mediated neurite outgrowth in PC12 cells via MEK/ERK and PI3K-Akt signaling pathways. *Food & Function*, *5*, 3160–3169.

Raman, J., Lakshmanan, H., John, P. A., Zhijian, C., Periasamy, V., David, P., Naidu, M., & Sabaratnam, V. (2015). Neurite outgrowth stimulatory effects of myco synthesized AuNPs from *Hericium erinaceus* (bull.: Fr.) Pers. on pheochromocytoma (PC-12) cells. *International Journal of Nanomedicine*, *10*, 5853–5863.

Ratto, D., Corana, F., Mannucci, B., Priori, E. C., Cobelli, F., Roda, E., Ferrari, B., Occhinegro, A., di Iorio, C., de Luca, F., Cesaroni, V., Girometta, C., Bottone, M. G., Savino, E., Kawagishi, H., & Rossi, P. (2019). *Hericium erinaceus* improves recognition memory and induces hippocampal and cerebellar neurogenesis in frail mice during aging. *Nutrients*, *11*, 715.

Rossi, P., Cesaroni, V., Brandalise, F., Occhinegro, A., Ratto, D., Perrucci, F., Lanaia, V., Girometta, C., Orrù, G., & Savino, E. (2018). Dietary supplementation of lion's mane medicinal mushroom, *Hericium erinaceus* (Agaricomycetes), and spatial memory in wild-type mice. *International Journal of Medicinal Mushrooms*, *20*, 485–494.

Rupcic, Z., Rascher, M., Kanaki, S., Koster, R. W., Stadler, M., & Wittstein, K. (2018). Two new cyathane diterpenoids from mycelial cultures of the medicinal mushroom *Hericium erinaceus* and the rare species, *Hericium flagellum*. *International Journal of Molecular Sciences*, *19*, 740.

Schindelin, J., Arganda-Carreras, I., Frise, E., Kaynig, V., Longair, M., Pietzsch, T., Preibisch, S., Rueden, C., Saalfeld, S., Schmid, B., Tinevez, J. Y., White, D. J., Hartenstein, V., Eliceiri, K., Tomancak, P., & Cardona, A. (2012). Fiji: An open-source platform for biological-image analysis. *Nature Methods*, *9*, 676–682.

Subedi, L., Cho, K., Park, Y. U., Choi, H. J., & Kim, S. Y. (2019). Sulforaphane-enriched broccoli sprouts pretreated by pulsed electric fields reduces neuroinflammation and ameliorates scopolamine-induced amnesia in mouse brain through its antioxidant ability via Nrf2-HO-1 activation. *Oxidative Medicine and Cellular Longevity*, *2019*, 3549274–3549219.

Tsai-Teng, T., Chin-Chu, C., Li-Ya, L., Wan-Ping, C., Chung-Kuang, L., Chien-Chang, S., Chi-Ying, H. F., Chien-Chih, C., & Shiao, Y. J. (2016). Erinacine A-enriched *Hericium erinaceus* mycelium ameliorates Alzheimer's disease-related pathologies in APPswe/PS1dE9 transgenic mice. *Journal of Biomedical Science*, *23*, 49.

Ustun, R., & Ayhan, P. (2019). Regenerative activity of *Hericium erinaceus* on axonal injury model using *in vitro* laser microdissection technique. *Neurological Research*, *41*, 265–274.

Vigna, L., Morelli, F., Agnelli, G. M., et al. (2019). *Hericium erinaceus* improves mood and sleep disorders in patients affected by overweight or obesity: Could circulating pro-BDNF and BDNF be potential biomarkers? *Evidence-Based Complementary and Alternative Medicine*, *2019*, 7861297.

Wang, T., Li, W., Martin, S., Papadopulos, A., Joensuu, M., Liu, C., Jiang, A., Shamsollahi, G., Amor, R., Lanoue, V., Padmanabhan, P., & Meunier, F. A. (2020). Radial contractility of actomyosin rings facilitates axonal trafficking and structural stability. *The Journal of Cell Biology*, *219*, e201902001.

Wang, T., Martin, S., Nguyen, T. H., Harper, C. B., Gormal, R. S., Martínez-Mármol, R., Karunanithi, S., Coulson, E. J., Glass, N. R., Cooper-White, J. J., van Swinderen, B., & Meunier, F. A. (2016). Flux of signalling endosomes undergoing axonal retrograde transport is encoded by presynaptic activity and TrkB. *Nature Communications*, *7*, 12976.

Wang, T., Martin, S., Papadopulos, A., Harper, C. B., Mavlyutov, T. A., Niranjan, D., Glass, N. R., Cooper-White, J. J., Sibarita, J. B., Choquet, D., Davletov, B., & Meunier, F. A. (2015). Control of autophagosome axonal retrograde flux by presynaptic activity unveiled using botulinum neurotoxin type a. *The Journal of Neuroscience*, *35*, 6179–6194.

Wittstein, K., Rascher, M., Rupcic, Z., Lowen, E., Winter, B., Koster, R. W., & Stadler, M. (2016). Corallocins A-C, nerve growth and brain-derived neurotrophic factor inducing metabolites from the mushroom *Hericium coralloides*. *Journal of Natural Products*, *79*, 2264–2269.

Wong, K. H., Naidu, M., David, R. P., Bakar, R., & Sabaratnam, V. (2012). Neuroregenerative potential of lion's mane mushroom, *Hericium erinaceus* (bull.: Fr.) Pers. (higher basidiomycetes), in the treatment of peripheral nerve injury (review). *International Journal of Medicinal Mushrooms*, *14*, 427–446.

Xiu, M. H., Hui, L., Dang, Y. F., Hou, T. D., Zhang, C. X., Zheng, Y. L., Chen, D. C., Kosten, T. R., & Zhang, X. Y. (2009). Decreased serum BDNF levels in chronic institutionalized schizophrenia on long-term treatment with typical and atypical antipsychotics. *Progress in Neuro-Psychopharmacology & Biological Psychiatry*, *33*, 1508–1512.

Zhang, C. C., Yin, X., Cao, C. Y., Wei, J., Zhang, Q., & Gao, J. M. (2015). Chemical constituents from *Hericium erinaceus* and their ability to stimulate NGF-mediated neurite outgrowth on PC12 cells. *Bioorganic & Medicinal Chemistry Letters*, *25*, 5078–5082.

Zhang, Z., Liu, X., Schroeder, J. P., Chan, C. B., Song, M., Yu, S. P., Weinshenker, D., & Ye, K. (2014). 7,8-dihydroxyflavone prevents synaptic loss and memory deficits in a mouse model of Alzheimer's disease. *Neuropsychopharmacology*, *39*, 638–650.

Zuccato, C., & Cattaneo, E. (2009). Brain-derived neurotrophic factor in neurodegenerative diseases. *Nature Reviews. Neurology*, *5*, 311–322.

SUPPORTING INFORMATION

Additional supporting information can be found online in the Supporting Information section at the end of this article.

How to cite this article: Martínez-Mármol, R., Chai, Y., Conroy, J. N., Khan, Z., Hong, S.-M., Kim, S. B., Gormal, R. S., Lee, D. H., Lee, J. K., Coulson, E. J., Lee, M. K., Kim, S. Y., & Meunier, F. A. (2023). Hericerin derivatives activates a pan-neurotrophic pathway in central hippocampal neurons converging to ERK1/2 signaling enhancing spatial memory. *Journal of Neurochemistry*, *00*, 1–18. https://doi.org/10.1111/jnc.15767